Journal of Biomedical Optics

SPIEDigitalLibrary.org/jbo

Review of fiber-optic pressure sensors for biomedical and biomechanical applications

Paulo Roriz
Orlando Frazão
António B. Lobo-Ribeiro
José L. Santos
José A. Simões

Journal of Biomedical Optics 18(5), 050903 (May 2013)

REVIEW

Review of fiber-optic pressure sensors for biomedical and biomechanical applications

Paulo Roriz,[a,b] Orlando Frazão,[b] António B. Lobo-Ribeiro,[b,c] José L. Santos,[b] and José A. Simões[a]
[a]University of Aveiro, Department of Mechanics, 3810-193 Aveiro, Portugal
[b]INESC-Porto and Faculty of Sciences of the University of Porto (FCUP), Rua do Campo Alegre, 687, 4150-179, Porto, Portugal
[c]University of Fernando Pessoa, Faculty of Health Sciences, Rua Carlos da Maia 296, 4120-150, Porto, Portugal

Abstract. As optical fibers revolutionize the way data is carried in telecommunications, the same is happening in the world of sensing. Fiber-optic sensors (FOS) rely on the principle of changing the properties of light that propagate in the fiber due to the effect of a specific physical or chemical parameter. We demonstrate the potentialities of this sensing concept to assess pressure in biomedical and biomechanical applications. FOSs are introduced after an overview of conventional sensors that are being used in the field. Pointing out their limitations, particularly as minimally invasive sensors, is also the starting point to argue FOSs are an alternative or a substitution technology. Even so, this technology will be more or less effective depending on the efforts to present more affordable turnkey solutions and peer-reviewed papers reporting *in vivo* experiments and clinical trials. [DOI: 10.1117/1.JBO.18.5.050903]

Keywords: fiber-optic sensors; pressure; biomechanics; biomedical.

Paper 130031VR received Jan. 20, 2013; revised manuscript received Apr. 15, 2013; accepted for publication Apr. 18, 2013; published online May 30, 2013.

1 Introduction

In the coming years, *in vivo* biomedical and biomechanical applications will benefit from a wide range of fiber-optic sensor (FOS) turnkey systems for sensing and measuring almost any physical quantity. These systems have four basic components: the light source, the optical fiber (OF), the sensor element, and the light detector. The light source provides the electromagnetic radiation whose energy is transmitted through the OF to the sensor element, in general, under the principle of total internal reflection. The FOS or transducer is the light modulator, i.e., the entity that causes a light property to change (e.g., amplitude or optical power, phase, polarization, and wavelength or optical frequency) under the influence of a certain physical quantity. Thus a physical quantity (e.g., pressure) can change the physical properties of the sensing element, which, in turn, leads to a change in the light properties. The light detector is necessary to read and analyze a light property variation. Since the four light properties can be considered in most circumstances independent parameters, they offer a wide range of solutions to sense several physical quantities.

Fiber-optic sensing technology is about forty years old and presents substantial advantages compared to conventional electric sensing systems. Conventional sensors applied in biomedical and biomechanical applications are based on piezoresistive, strain gauge (SG), or other solid-state sensing technologies. They represent a highly tested, mature and overspread technology, offering good sensitivity, precise measurements, and competitive price. However, their miniaturization, typically requiring sensor head diameters below 0.5 mm, such as for minimally invasive procedures, presents some drawbacks. Mignani and Baldini[1] have pointed out some of them, including fragility, long-term instability, inconsistency, and excessive drift. Additionally, their output is restricted to a small sensing area making it necessary to use more sensors to sense larger regions (e.g., a temperature profile along a tissue), but only at the expense of increased dimensions and loss of flexibility.[2] These disadvantages combined with poor biocompatibility of metallic components and large sensitivity to electromagnetic interference (EMI) can compromise some *in vivo* applications and their use in clinical practice. A good example is their application in magnetic resonance imaging (MRI) environment. As pointed by Ladd and Quick[3] ferromagnetic based sensors should not be used because they will act as an antenna and generate significant heating effects, which might cause image artifacts.

While OFs guide light, the majority of conventional sensors guide electricity through metallic wires (e.g., copper-nickel alloys). This fundamental difference of carrying information, along with the following properties, makes OF the tool of choice in an increasing number of sensing environments:

- *Inertness and biocompatibility*: A typical OF is made of amorphous silica glass, also known as silicon dioxide (SiO_2), fused silica, or fused quartz. This compound is almost chemically inert and biocompatible.[4] Only hydrofluoric acid and some alkaline substances are capable to chemically attack it.[5,6] Thus an OF has the potential to not adversely affect the physiological environment nor be adversely affected by it.[7] Under sterile conditions, OF will minimize contamination and the risk of infection associated to invasive procedures. Even so, there is a need of special care to glass debris that can be generated along with fiber breakage. Sharpened glass pieces can easily lacerate the skin, enter to the circulatory system, or damage internal body cells and tissues. One should remember that some materials are biocompatible in their bulk form, but wear debris can incite adverse reactions

Address all correspondence to: Orlando Frazão, INESC-Porto and Faculty of Sciences of the University of Porto (FCUP), Rua do Campo Alegre, 687, 4150-179, Porto, Portugal. Tel: +351-220-402-301; Fax: +351-220-402-437; E-mail: ofrazão@inescporto.pt

from the body cells. To avoid it, the OF is usually embedded into biocompatible and sterilizable protective layers, such as coatings, buffers, jackets, and cables. Materials such as polyimide, polydimethylsiloxane (PDMS), ethylene-tetrafluoroethylene or Tefzel®, and polytetrafluoroethylene (PTFE) or Teflon® are being used in biomedical and biomechanical applications.[8–13] The strength, fatigue, and biocompatibility of silica fibers with several polymeric (e.g., UV-cured acrylate, silicone, and polyimide), metallic (e.g., aluminum, indium, tin, and gold) and inorganic (e.g., oxides, carbides, nitrides, and carbon) coatings were studied by Biswas.[9] The UV-curable dual acrylate coating used in standard OF may be inappropriate for biomedical and biomechanical applications requiring heating procedures because it cannot withstand temperatures above 85°C.[14] Some manufacturers, such as Ocean Optics (Dunedin, Florida; www.oceanoptics.com) and OFS (Norcross, Georgia; www.ofsoptics.com), are producing nontoxic and biocompatible fibers, cables, and assemblies, with materials used in implants and/or approved by the United States Pharmacopeia (USP Class VI Biological Test for Plastics). Some examples of these materials are polyetheretherketone, fluoroacrylates, Poly(*p*-xylylene) or parylene, and polyimide. The OF can also be enclosed or encapsulated into surgical instruments, catheters, metallic tubes, or needles. These objects play several cumulative functions such as guide the FOS to the target during invasive procedures, protect the sensor or the host from direct contact, allow exposure of the sensing head only, minimize the risk of sensor breakage and the release of debris, or incorporate additional sensors and devices.[10,15–21] While almost all needles and metallic tubes are made of stainless steel, catheters can be made from a wide variety of materials, such as silicone rubber, latex, PTFE or Teflon, polyethylene, polyurethane, polyethylene, and polyvinyl chloride.

- *Low coefficient of thermal expansion and thermal conductivity*: The coefficient of thermal expansion of an OF is 1/34 of copper.[22] This low sensitivity minimizes cross sensitivity in the sensor probe. In addition, the operating temperature of a silica fiber can go up to ~900°C, above which the core and the cladding material begin to migrate. Thus an OF will not lose its integrity with body temperature monitoring, especially during hyperthermia or cryotherapy treatments. In fact, the critical issue relies on the selection of high temperature resistant layers for coating, buffering and cabling. Some recommended high-temperature-resistant polymers are Teflon/PTFE (230°C), polyimide (220°C), and silicone rubber (200°C).[16] Other materials with higher melting points, such as sapphire (2040°C) and silicon carbide (2700°C), can even replace silica based OF.[22]
- *No electrical conductivity*: An OF has excellent electrical insulation, up to ~1000°C.[22–24] Thus it is intrinsically safer to be used in animals or patients without the risk of electrical shock or explosion.
- *Immunity to EMI*[23,25]: The dielectric properties offered by OF will maximize the signal-to-noise ratio and the sensitivity of any FOS system. Of particular importance is the possibility of using the OF in MRI rooms.
- *Remote operation and sensing*: An OF is capable of transmitting a large amount of data over long distances (several kilometers) at the speed of light without significant signal loss (typically <0.4 dB km^{-1}).[23,25]
- *Small dimensions and lightweight*: The OF is very thin, no thicker than a standard surgical suture.[26] A typical single mode fiber (SMF) has an outer diameter (OD) of only 125 μm. Supplementary protective layers will increase dimensions, but to no more than 500 μm OD if minimally invasive procedures are pursued. The OF is also lightweight. SiO_2 density (2200 kg m^{-3}) is approximately four times smaller than that of copper,[22] which also facilitates miniaturization.
- *Adhesion to biological tissues*: An OF can easily adhere to bone by use of the US Food and Drug Administration (FDA) approved polymethyl-methacrylate (PMMA) as bonding adhesive.[26] This is of particular importance for *ex vivo* biomechanical experiments where bone strains need to be assessed.
- *Geometrical versatility*: An OF can bend within the host structure to radii of 10 mm,[23] making it suitable to adapt to complex surfaces, such as skin, teeth, joint, and bone surfaces.[27]

An OF is only a component of FOS systems, but its unique properties definitely contribute to enhance the performance of the whole system and to claim FOS as a standard for sensing and capable of providing reliable solutions for those applications where conventional sensors are not suitable.

FOS were introduced in the 1960s, mainly for endoscopic, intravascular, and cardiac applications.[28–42] In the last years, their expansion has been benefiting from the development of telecommunications and OF communications, in particular, which are offering high-quality, miniaturized, and affordable optoelectronic components at competitive prices.

The most common working principles applied to FOS for biomedical and biomechanical applications are based on intensity, phase, and wavelength modulation, the latter associated with the operation of fiber Bragg gratings (FBG).

Intensity modulated sensors were introduced in the early 1960s.[29–42] Their working principle is based on the variation of the light intensity or amplitude. Some possible configurations have been described:[43,44] an OF placed in front of a movable and reflecting mirror (Fig. 1). The fiber guides the light to the mirror. The measurand varies the original mirror distance to the fiber tip and changes the intensity of the reflected light that is coupled by the same fiber or another fiber parallel to the first one. As will be described, initial studies made use of similar configurations. However, instead of a single OF, bundles of OF and non-fiber-optical components were used as waveguides due to problems in light coupling that time;[29–42,45] two OF in front of each other at a known distance (Fig. 2). The measurand will change the distance between the two fibers and, consequently, the intensity transmitted. Differential configurations, with two or more fibers in front of the OF connected to the light source, can compensate changes in light source intensity or losses in the OF (Fig. 3); an OF submitted to macrobending (Fig. 4) or microbending (Fig. 5). These actions will result in light loss and decrease the light intensity output.[46]

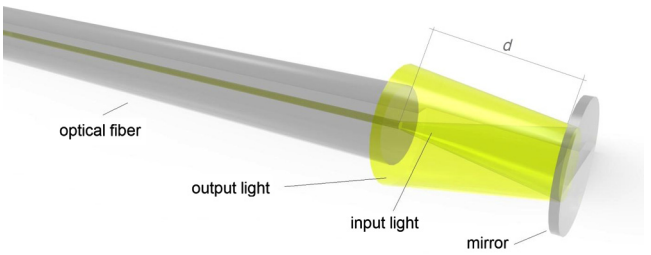

Fig. 1 Schematic drawing of an optical fiber (OF) placed in front of a movable reflecting mirror. The back-reflected intensity decreases when the distance, d, between the OF and the mirror increases.

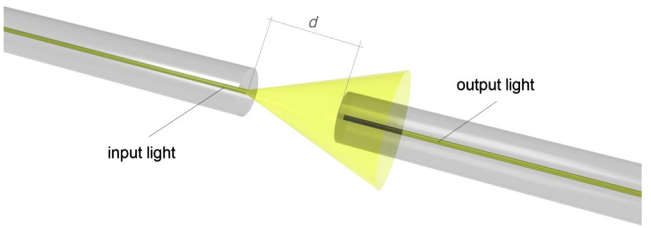

Fig. 2 Schematic drawing of two OFs in front of each other at a known distance (d). The transmitted intensity decreases when the distance, d, increases.

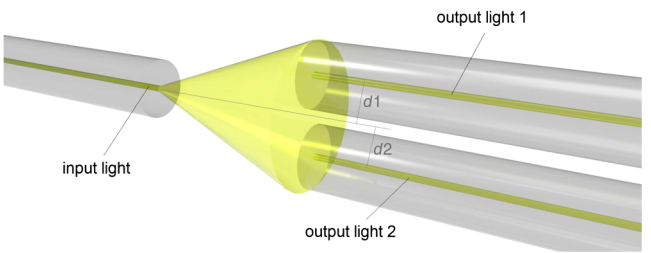

Fig. 3 Schematic drawing of a differential configuration. The input light from one OF is coupled by the two OF. If the distances, d1 and d2, between the longitudinal axis of the input OF and the corresponding longitudinal axes of the two output OF increase the transmitted intensity decreases.

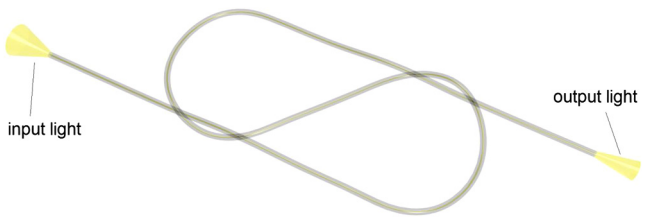

Fig. 4 Schematic drawing of a typical macrobending configuration (figure-of-eight loop). A variation of elongation applied to both fiber ends is converted into a variation of curvature radius of both loops, causing the macrobending light loss effect.

Interferometric-based sensors also made several configurations possible (e.g., Sagnac interferometer, Michelson interferometer, Mach-Zehnder interferometer), but the Fabry-Pérot (F-P) interferometer[47] has been the most applied in minimally invasive sensors. F-P interferometer sensors were introduced in the early 1980s and solved many drawbacks of intensity-modulated sensors. Instead of measuring a change in light intensity, these sensors look to phase differences in the light beams.

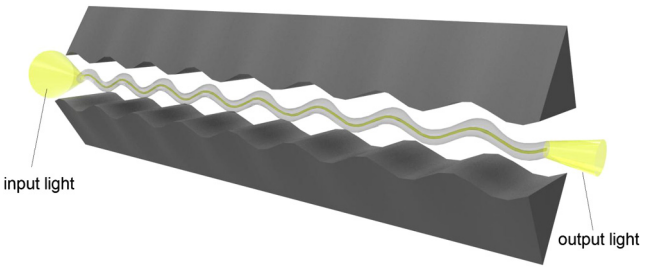

Fig. 5 Schematic drawing of a microbend configuration. The optical power leakage is a function of the microbend radio of curvature which may be induced by strain or force applied along the fiber length.

Their most common configuration includes a small-size sensing element bonded to the tip of the fiber. This element is an optical cavity formed by two parallel reflecting surfaces where multiple reflections will occur (Fig. 6). One of the reflecting surfaces is a diaphragm that changes the optical cavity depth (i.e., the distance between the mirrors) under the action of the measurand and, consequently, the characteristics of the signal that reaches the photodetector. Compared with intensity modulated schemes and FBG sensors, F-P interferometers are capable of achieving high sensitivities and resolutions, but at the expense of relatively complex interrogation/detection techniques.[48]

Wavelength modulation is typically achieved through use of FBG sensors. A Bragg grating can be defined as a periodic perturbation of the refractive index of the fiber core (Fig. 7). Several disruptive discoveries have to occur to make their use as sensors possible. The first one in 1978 was the discovery of

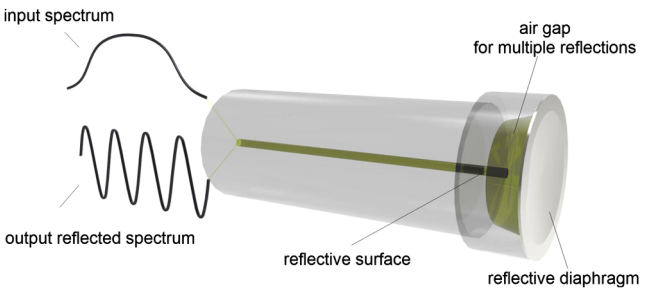

Fig. 6 Schematic drawing of a typical Fabry-Pérot (F-P) configuration that can be used for pressure measurements.

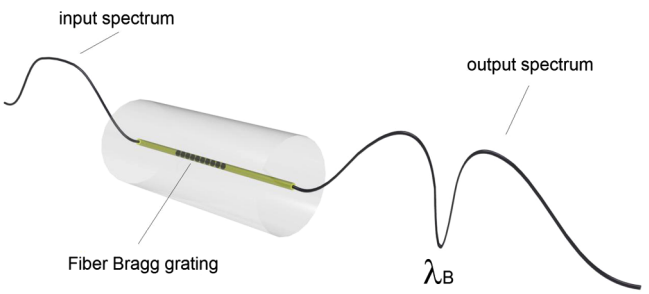

Fig. 7 Schematic drawing of a fiber Bragg grating (FBG). The grating acts as an effective optical filter. When illuminated by a broadband optical source, whose center wavelength is close to the Bragg wavelength (λB), a narrow band loss centered in the Bragg wavelength is present in the transmitted spectrum (the missing light appears in the grating reflection spectrum).

photosensitivity in OF by Hill et al.[49,50] In 1987 it was followed by the invention of the externally UV photowriting technique, by Meltz et al.[51] In fact, it was this new transverse holographic UV photowriting technique of inscribing Bragg gratings into the core of OF with high concentration of core Ge-doping that contributed to the growth of FBG devices in the R&D telecom and sensing communities.[52] Their working principle is based on the reflection of light, at the Bragg wavelength (λ_B), when the OF is illuminated by a broadband source whose center wavelength is close to the Bragg wavelength. When the fiber is stretched or compressed along its axis, the refractive index will change (photo-elastic effect) along with the spacing between the grating lines (i.e., the grating period or grating pitch). Because the Bragg wavelength is directly proportional to the grating period, a shift in the Bragg wavelength will be observed making possible to monitor the induced strain.[53] The sensitivities for strain and temperature of a FBG recorded at 1550 nm are approximately 1.2 pm $\mu\varepsilon^{-1}$ and 13.7 pm °C^{-1}, respectively.[53]

The possibility of multiplexing these structures is also revolutionizing the world of sensing. With time division multiplexing and wavelength division multiplexing (WDM) or switching, hundreds of in-line FBG sensors can be read with a single decoder unit.[25,54–56] As an example, considering strain, about 33 FBG sensors can be accommodated in a 50 nm spectrum using a Bragg wavelength spacing between 2 and 4 nm and taking into account each FBG is allowed an independent strain range of ±500 and a 250 $\mu\varepsilon$ guard band.[57] Additionally, multiplexing will also contribute to reduce the cost per sensor and of the whole system making FBG competitive with conventional sensors.[58] Compared with conventional sensors, namely the foil SG, FBG sensors are capable of providing absolute strain measurements with easier instrumentation.[53] They also offer an excellent measurand-type range and can be used as a generic sensing element to quantify other physical quantities (e.g., force, acceleration, pressure, vibration, electromagnetic field, etc.) and certain chemical quantities.[59,60]

Some of the ideas just presented seem to be appellative. However, FOS remains unknown to many engineers, clinicians, and researchers. Most probably because engineering courses and research are focused on conventional sensors and nonoptical technologies. On the other hand, there is a relatively small number of turnkey solutions as well as companies and retailers commercializing these devices, which may justify their limited wide spreading. Even so, some companies are offering customer-specified or plug-and-play sensing solutions specifically for biomedical and biomechanical applications (Table 1). Some of them will benefit from small or handheld interrogators, capable of minimizing patient discomfort during continuous day-to-day monitoring.[61] Others will require more comparative studies, particularly *in vivo* experiments and clinical trials to clearly state their potentialities. In fact, an important drawback of some FOS is the lack of scientific information (e.g., peer-reviewed papers) reporting their use in clinical practice. Probably, they are being used but without the necessity of writing a paper or putting the brand name on it. The absence of detailed technical specifications (e.g., repeatability, reproducibility, working range, accuracy, resolution, and response time) was also detected in some published papers that report use of commercial solutions, particularly from nonoriginal equipment manufacturer (OEM) or reseller companies. Those benefiting from approvals of the American Association for Medical Instrumentation (AAMI), International Organization for Standardization

Table 1 Companies commercializing fiber-optic sensors (FOS) for biomechanical and biomedical applications.

Company	Local, country	Website
Arrow International, Inc.	Teleflex Medical, Research Triangle Park, North Carolina	www.arrowintl.com
BioTechPlex	Escondido, California	www.biotechplex.com
Camino Laboratories	San Diego, California	www.integralife.com
Endosense, SA	Geneva, Switzerland	www.endosense.com
FISO Technologies	Québec, Canada	www.fiso.com
InnerSpace Medical, Inc.	Tustin, California	www.innerspacemedical.com
InvivoSense	Trondheim, Norway	www.invivosense.co.uk
LumaSense Technologies	Santa Clara, California	www.lumasenseinc.com
Luna Innovations	Blacksburg, Virginia	www.lunainnovations.com
MAQUET Getinge Group	Rastatt, Germany	http://ca.maquet.com
Neoptix Inc.	Québec, Canada	www.neoptix.com
Opsens	Québec, Canada	www.opsens.com
Radi Medical Systems	Uppsala, Sweden	www.radi.se
RJC Enterprises, LLC	Bothell, Washington	www.rjcenterprises.net
Samba Sensors	Västra Frölunda, Sweden	www.sambasensors.com

(ISO), US FDA, or similar regional/country organizations will probably lead the market. Cost is also a critical issue. In fact, the high cost associated with some optoelectronic (e.g., integrated source and detector devices) and miniaturized solutions, developed to achieve the resolutions required for biomedical and biomechanical applications, can compromise their acquisition. A shared problem with almost all sensors is that FOS also suffer from interference of multiple effects or cross-sensitivity. A good example is that of FBG sensors, which present dual sensitivity to strain and temperature. Currently used compensation techniques are capable of minimizing erroneous readings or uncertainties from nondesirable effects. To enable secure readings, these techniques should always be implemented instead of assuming negligible effects under apparently controlled situations.

Finally, FOS are also competing with mature nonoptical technologies that seem capable of overcoming some of their traditional limitations. The most promising are microelectromechanical systems, which technology, along with examples and applications, is well described in the work of Polla et al.[62] and Voldman et al.[63] The Neurovent microchip SG catheter (Raumedic AG, Münchberg, Germany; www.raumedic.com) is a good example of a commercially available solution offering zero drift and MRI compatibility.[64–66] Semiconductor SGs, such as piezoresistive-based silicon devices, are also becoming competitive, particularly for micro-strain measurements. This powerful technology is offering linear mechanical and electrical response with negligible hysteresis and a relatively low temperature effect.[67]

In the following sections, a review effort presents the most relevant contributions of FOS to assess pressure in biomedical and biomechanical applications. Other interesting physical, chemical, or physiological parameters such as temperature, strain and force, or glucose, PH, gases and DNA were not addressed and can be found elsewhere.[44,61,68–77] Our approach to FOS has been carried out after a brief mention to conventional sensors and their limitations. Emphasis was given to description of *in vivo* experiments and clinical applications. Thus, we hope to have contributed for a better framework of FOS, pointing their advantages and triggering new ideas for those engaged in their development and application in the biomedical and biomechanical fields.

2 Fiber-Optic Pressure Sensors

Following some original works in the first half of the last century,[78–81] it was in the 1960s that interstitial fluid pressure monitoring became a relevant procedure in biomedical and biomechanical applications.[32,39,82–85] In the early 1970s, Millar Instruments Inc. (Houston, Texas; www.millarinstruments.com) made significant efforts to develop miniaturized piezoresistive pressure sensors and to integrate them into catheters for clinical practice.[86] These are currently known as the Millar Mikro-Tip® pressure transducer catheters. Their accuracy is ~0.2% but they are also fragile, expensive, and affected by EMI.[87,88]

Fluid-filled catheters attached to external pressure transducers can be used as an alternative to the previous solid-state sensors.[80,88,89] Early configurations such as a simple needle connected to a mercury pressure manometer[79] gave place to more advanced configurations, such as the wick catheter,[85,90] the slit catheter,[91] or the side-ported needle.[92] Nevertheless, besides low-cost, their performance seems to be lower than that of Millar catheters. According to the review of Kaufman et al.,[93] the accuracy of fluid-filled systems ranges between 1% and 18%, and their linearity between 2% and 15%. They also suffer from hydrostatic artifacts caused by body movements, limiting their use to static body positions or movements in the horizontal plane.[89,94] Furthermore, they require flushing or infusion to maintain accuracy, particularly during long-term measurements (i.e., more than 1 h).[95] Meanwhile, other fluid-filled catheter-transducers, such as the Spiegelberg intracranial pressure (ICP) monitoring system (Spiegelberg KG, Hamburg, Germany; www.spiegelberg.de) and the AirPulse™ Air Management System (InnerSpace, Tustin, California), have been developed and were capable to overcome the previous problems.[96]

FOS are intrinsically free from hydrostatic artifacts and flushing, making them attractive for interstitial fluid pressure measurements. Intensity modulated schemes were initially proposed, namely for *in vivo* blood pressure measurement, such as in the original work of Lekholm and Lindström[40,45] and other similar configurations.[39,97,98] The work of Lekholm and Lindström[40,45] was also the basis for development of Camino pressure sensors (Camino Laboratories, San Diego, California; acquired by Integra LifeSciences; Plainsboro, New Jersey, USA; www.integralife.com), probably the most widespread dual-beam referencing intensity-modulated-based sensors.[99] Camino sensors became popular in the 1980s, and since that time they have been extensively used for pressure measurement in different sites of the body, as in the brain, muscles, and joints. In 1996 Keck reported the company was producing around 60,000 devices/year.[52] They also underwent extensive scrutiny leading to identification of several drawbacks and questioning their routine use, particularly in clinical practice.[64,100–112]

To overcome some of the drawbacks of intensity-modulated sensors, alternative configurations have been presented. In the early 1980s, F-P interferometer-based sensors were introduced. An earlier configuration of a F-P sensor was presented in 1983 by Cox and Jones,[113] but large size and complex signal analysis limited further applications.[88] MetriCor Inc. (acquired by Photonetics, Inc.; at present part of GN Nettest, Copenhagen, Denmark; www.gnnettest.com) developed a compact version, based on anodic bonding of a silicon membrane to the fiber tip and use of two wavelengths to monitor the interferometer.[52,114] The same technology was adapted by Sira, Ltd. (Kent, UK; www.siraeo.co.uk) to measure temperature and the refractive index.[52] Innovation also came from miniaturized forms; namely, those using all-fused-silica designs and clean-room microfabrication techniques.[88,93,115]

Recently, FBG sensors have also been proposed to assess pressure; namely, in the nucleus pulposus of the intervertebral discs of the spine.[19,20,60,116] However, these apply only to *ex vivo* experiments. Thus, innovative solutions are mandatory for *in vivo* and clinical studies, namely to be integrated into specific diagnostic procedures of the spine (e.g., discometry) and surgical procedures (e.g., arthrodesis and arthroplasty).

Considering the wide variety of pressure FOS and their applications, a better framework can be obtained by looking at the specific pressure applications that have been developed. We expect to contribute to them in the following subsections.

2.1 *Intravascular and Intracardiac Pressure*

Among several experiments that started in the mid-1960s,[32,39,40,45] the original work of Lekholm and Lindström[40,45] deserves to be highlighted. A sensor intended for *in vivo* blood

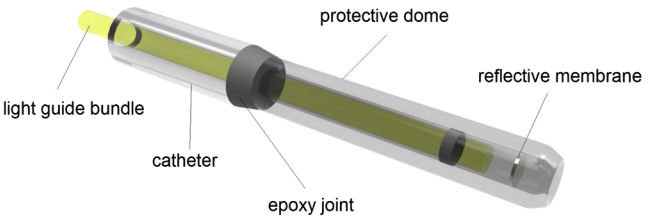

Fig. 8 Schematic drawing of the pressure sensor proposed by Lekholm and Lindström.[40,45]

pressure measurement with sensor heads of only 0.85-mm (unshielded) and 1.5-mm OD was proposed (Fig. 8). It consisted of an air-filled chamber covered by a 6 μm pressure-sensitive beryllium-copper membrane. As in similar works of that period,[29,39] the guiding system was made of two independent OF bundles. One bundle was used to guide the light from a gallium-arsenide light emitting diode (LED) source to the sensor head, the other to guide the reflected light into a photodetector.[45] The first fabricated probes had a flat frequency response from static pressure to about 200 Hz.[40] In later developments, a frequency response of flat to 15 kHz was measured in one of the fabricated probes.[45] A high-frequency response can be useful to obtain more accurate measurements, particularly if pressure artifacts caused by mechanical vibrations, shocks, and movements are present and to calculate accurate pressure derivatives.[117,118] In fact, this feature is claimed by current catheters, such as the Millar Mikro-Tip® catheter, which is capable of exhibiting a frequency response of flat to 10 kHz.[119] Even so, frequency responses up to 250 Hz seem to be sufficient for accurate measurements of blood pressure and pressure derivatives.[120–122] The sensor proposed by Lekholm and Lindström also exhibited zero drift under temperature variation from 20°C to 37°C, recovering the baseline after ~40 s.[45] Moreover, the sensor was extensively described, covering the theoretical topics of fiber-optic properties, membrane reflection, operation modes, number of fibers and their distribution, membrane mechanics, volume displacement, frequency dependence, and limitations.[45] Error sources, sensitivity and miniaturization, failure, and redundancy were also addressed.[45] Another interesting feature of the sensor was its insensitivity to mechanical vibrations, shocks, and movements due to a light and stiff membrane. After successful tests on one dog and one man,[40] clinical tests have followed.[45]

In the following years, similar sensors with vibrating membranes located at the tip[39,97,98] or at the side of a catheter have been proposed.[123,124] Side membranes should contribute to reduce pressure artifacts due to tip collisions with the blood vessels or the ventricular walls (the so-called wall or piston effect)[124–126] and to avoid clot formation occurring for long periods of monitoring.[123,124] An earlier application of a pressure sensor incorporating a side membrane was proposed by Matsumoto et al.[124] (Fig. 9). Nevertheless, tip and side-hole configurations have been adopted up to today. In fact, the most important achievement in the following years was the implementation of microfabrication techniques.[127–131]

The configuration proposed by Lekholm and Lindström[40,45] was also the basis for the development of Camino pressure sensors (San Diego, California). This transducer-tipped catheter consisted of a 1.35-mm OD tip enclosed in a saline-filled sheath (2.1-mm OD) with side holes (Fig. 10). A pressure-sensitive diaphragm caused the mirror distance from the fiber tip to vary, changing the intensity of the reflected light. As will be seen,

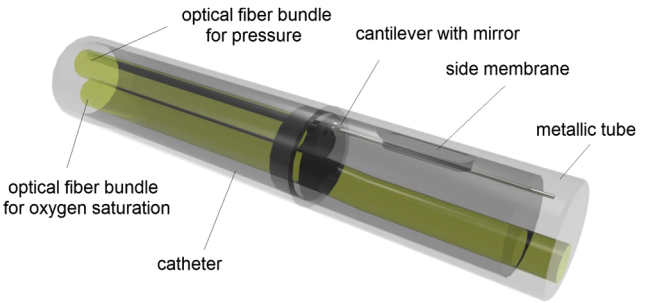

Fig. 9 Schematic drawing of the pressure and oxygen saturation sensor proposed by Matsumoto et al.[124] A side membrane was used to sense pressure and a tip configuration for measurement of oxygen saturation.

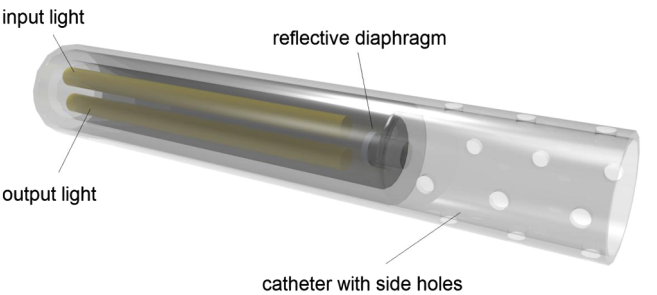

Fig. 10 Schematic drawing of earlier Camino sensors.[89]

identical designs were also applied to measure intramuscular,[89] intraarticular,[132–135] and intracranial pressures.[136]

These transducers are interrogated by the intensity-modulation technique with dual-beam referencing, recommended for single use, and should not be resterilized or reused.[99] They are also relatively large (1.35-mm OD) and require special handling due to potential for fiber breakage.[100,102]

Several alternative configurations to the above sensors were presented; namely, those based on the photo-elastic effect.[137] It was, however, the introduction of F-P sensors that made it possible to incorporate important features.[113] The LED-microshift sensor proposed by Wolthuis et al.[88,138,139] is a good example (Fig. 11). It consisted of a glass cube ($300 \times 300 \times 275$ μm) containing a thin F-P cavity (1.4 to 1.7 μm depth; 200 μm OD) covered by a pressure sensitive single crystal silicon diaphragm anodically bonded to the glass cube. A LED, with an emission bandwidth of ~60 nm, was used to interrogate the cavity operating within a single reflectance cycle. A dichroic ratio technique was applied to analyze the reflected light. A linear pressure working range from 500 to 1100 mmHg (absolute) was achieved. Sensor's resolution (<1 mmHg) and accuracy

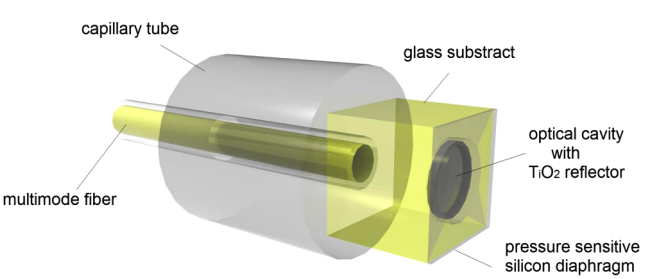

Fig. 11 Schematic drawing of the pressure sensor proposed by Wolthuis et al.[88,138]

(±1 mmHg) fulfilled AAMI medical standards. It was validated using a Millar Micro-tip® catheter and proposed for absolute pressure measurements of the left heart chamber and systemic arterial pressures. The system was also low cost and easy to fabricate.[88] Wolthuis et al.[140] also have proposed a dual-function sensor system for simultaneous measurement of pressure and temperature. RJC Enterprises, LLC (Bothell, Washington) is commercializing these type of sensors; namely for resellers. For example, the pressure sensor has been integrated in the intra-aortic balloon (IAB) catheter of Arrow International, Inc. (Teleflex Medical, Research Triangle Park, North Carolina).[139]

Recently, another F-P sensor was successfully tested *in vitro* and proposed for continuous flow left ventricular assist devices (LVAD).[141] The F-P cavity consisted of a biocompatible parylene diaphragm and a silicon mirror fabricated directly on the inlet shell of the LVAD device. Sensor sensitivity (1 mmHg achieved by fringe counting; less than 0.1 mmHg with interpolation), linear range (up to 100 mmHg) and response time (1 ms; limited by the response time of the optical detector and the self-resonance frequency of the parylene-C membrane) meet the requirements of LVAD pressure-sensing systems.[141] Nevertheless, further improvements are mandatory for animal and human testing. In this case, however, authors have pointed the necessary steps to accomplish it.[141]

Several companies, such as FISO Technologies (Québec, Canada), Arrow International, Inc. and MAQUET Getinge Group (Rastatt, Germany), are providing F-P based sensors to monitor the arterial pressure during IAB pump therapy. FISO Technologies is recommending the fiber optic pressure (FOP)-MIV sensor (550 μm OD).[122] According to manufacturers' specifications, it has a measurement range from −300 to 300 mmHg, an accuracy of 1.5% (or ±1 mmHg) of full-scale output (FSO), a resolution better than 0.3 mmHg, a thermal effect sensitivity of $-0.05\%\,°C^{-1}$ and a zero drift thermal effect of -0.4 mmHg $°C^{-1}$ (Ref. 21). It was also demonstrated that *in situ* pressure monitoring with these sensors is more accurate and safer than external pressure monitoring through fluid-filled catheters.[142] Yet to our best knowledge, FOP-MIV has been used to measure the left ventricular pressure uniquely in animals.[143] Other applications of the same sensor, still with animals, included measurement of intracranial,[144,145] intraocular,[146] and intramedullary pressures.[147] A human *in vivo* application was reported for deglutition analysis assessed by measurement of pharyngeal pressure.[148] Arrow International Inc. commercializes the FiberOptix™ IAB Catheter, used in clinical practice to monitor arterial pressure.[139,149] MAQUET Getinge Group is commercializing two IAB catheters (Sensation Plus™ 8Fr. 50 cc IAB Catheter and Sensation® 7Fr. IAB Catheter), both allowing *in vivo* calibration and recalibration.[150] Unfortunately, we were unable to found further scientific or technical data (e.g., pressure range, accuracy, resolution, and response time) for the above sensors.

Frequently, the F-P cavity is bonded to the OF tip.[148,151] Typically, with this type of extrinsic configuration, the tip diameter is larger than that of the OF, which may represent a limitation concerning further miniaturization. Yet new approaches are contributing to enhance the potential of miniaturization offered by FOS.[115,152–155] Totsu et al.[115,152] have presented a sensor of only 125 μm OD to monitor pressure in the heart and aorta of a goat. The F-P cavity (~2 μm depth) was composed of two mirrors, a chromium half-mirror located at the tip of a multimode fiber (MMF), and an aluminum mirror in the head of the sensor. The head of the sensor was made of a thin SiO_2 diaphragm with a mesa (to support the mirror) and a polyimide spacer that was bonded to the MMF. Cleanroom microfabrication techniques were applied to produce the probe, in particular plasma-enhanced chemical vapor deposition, atmospheric pressure chemical vapor deposition, evaporation in vacuum, spin-coating, and deep reactive-ion etching (RIE). The system included a white light source, a fiber coupler, and a spectrometer. White light interferometry was used to avoid error and noise caused by bending of the OF and fluctuation of the light source. Sensor exhibited a pressure working range from −100 to 400 mmHg and a resolution of 4 mmHg.[115,152] A slightly different vacuum sealed F-P cavity technique was proposed for temperature compensation.[152]

Cibula et al.[154,155] were also capable of presenting a similar sensor (125 μm OD). In this case the diaphragm was designed to be a part of the OF, because the bonding process used in the work of Totsu et al.[115,152] limited the temperature range and sensor long-term stability.[155] The F-P cavity was created at the tip of the fiber by chemical etching. The diaphragm, made of polymer, was laid over the tip cavity by a "dip and evaporate" technique.[154] Several prototypes were presented with resolution of 10 Pa and pressures ranging from 0 to 40 kPa and from 0 to 1200 kPa. An all-fused-silica design, based on the replacement of the polymer diaphragm by a silica one, was also proposed.[153] This approach changed resolution to 300 Pa.

The advantage of all-fused-silica fabrication techniques (e.g., splicing, cleaving, and wet etching) is their low-cost. However, mass production may be compromised due to a large number of production steps, including fusion splices, precision cleaves, and micrometer length adjustments of the spliced fiber segments.[155] Significant efforts are being made to reduce some of these critical and time-consuming steps. That is the case of time-controlled chemical etching, which eliminates precision length adjustments of critical sensor constituents and improves sensor sensitivity.[155] Future trends should include biomechanical and biomedical applications. Meanwhile, FISO Technologies (Québec, Canada) has already claimed the smallest (125 μm OD) all-glass commercially available sensor (FOP-F125) for human body fluid pressure measurements.[156,157] Depending on the pressure range, the accuracy of the sensor varies from ±5 mmHg (−25 to +125 mmHg) to ±8 mmHg (−300 to +300 mmHg). Its resolution is better than 0.4 mmHg. The sensitivity thermal effect is of $0.1\%\ °C^{-1}$ and the zero thermal effect of 0.4 mmHg $°C^{-1}$. Proof pressure is of 600 mmHg and the operating temperature is between 10°C and 50°C.[157]

2.2 *Intramuscular or Intracompartmental Pressure*

Intramuscular pressure (IMP) is defined as the hydrostatic fluid pressure within a muscle.[158] Its measurement is of particularly importance for diagnosis of acute and chronic (muscle) compartment syndromes.[89,94,95] IMP is directly correlated with the force output of the muscle.[158,159] Therefore, by measuring IMP, the contribution of an individual muscle group to the force measured over a joint can be assessed.

Crenshaw et al.[89,95] were the first to use fiber-optic transducer-tipped catheters (model 110, Camino Laboratories, San Diego, California) to measure IMP. The accuracy and reliability of the system were validated trough a comparison with a slit catheter.[89] Preliminary tests also indicated their ability to continuously measure pressures ranging from 0 to 250 mmHg for a three day period. Experiments were made in animal and

human volunteers.[89] These sensors prove to be insensitive to hydrostatic artifacts caused by body movements and capable of long-term measurements (~2.5 h) without the necessity of flushing to maintain accuracy. Conversely, long-term measurements were also associated with patient discomfort, probably due to the size and rigidity of the polyethylene sheath enclosing the sensor.[89] Even so, these sensors were extensively used for IMP measurements, such as during isometric and concentric exercises,[95] to demonstrate that IMP varies with muscle depth,[160] to study compartment syndrome following prolonged pelvic surgery[161] and to analyze muscles contribution during gait.[94]

To accomplish the requirements of miniaturization for minimally invasive procedures Kaufman et al.[93] proposed a new fiber-optical microsensor with 360 μm OD (Luna Innovations, Blacksburg, Virginia). Even so, a too large diameter compared with muscle fibers diameters (between 57 and 73 μm).[162] The sensor consisted of an extrinsic F-P air cavity in-between a polished end fiber and a reflective membrane.[93,163] It was calibrated inside an air-pressure chamber under slowly dynamic pressures ranging from 0 to 250 mmHg back to 0 mmHg, over a period of 120 s. The output was compared with that of a reference sensor (Model PX5500, Omega Engineering Inc., Stanford, Connecticut; www.omega.com). Sensor's accuracy, repeatability, and linearity were better than 2% FSO, hysteresis of 4.5% FSO and sampling frequency of 66 Hz (~10 Hz with eight channels). Its accuracy was better than most of the fluid-filled systems (between 1% and 18%), but smaller than electronic transducer-tipped catheters (0.2% accuracy).[164] Despite that, the small diameter and immunity to electromagnetic fields prevailed.[93] Following functional characterization, the sensor was evaluated for biocompatibility using ISO standard 10993-6:2007 (Tests for Local Effects After Implantation).[165] *In vivo* experiments took place to measure IMP in the tibialis anterior muscle of anesthetized rabbits[166] and swine intra-myocardial pressure.[167] In the former study, a fluid pressure chamber was used to calibrate the sensor under sinusoidal pressure variation around a static pressure of ~60 mmHg. Reproducibility was possible only with degassed water, but unpredictable results were obtained with tap water. Calibration frequencies varied from 0.5 to 10 Hz, and the output was compared with that of a reference sensor (Millar Instruments, Inc., Houston, Texas). Hysteresis was not significant (4.5% FSO). Sensor sensitivity was 8.78 mV mmHg^{-1} remaining flat at 6 Hz and presenting a slightly decrease from 6 to 10 Hz. A slightly lower sensitivity was registered at 23°C than at 37°C, suggesting a possible, but smaller, temperature effect. A constant time delay of 130 ms was also registered probably due to postprocessing electronics. Phase delay was independent of temperature and increased linearly with frequency. Sensor also demonstrated excellent reproducibility during tests of two consecutive days.[167] A second-generation sensor (Luna Innovations, Blacksburg, Virginia) with smaller OD (250 to 280 μm), similar accuracy ($1.45 \pm 0.32\%$) and repeatability ($1.5 \pm 0.81\%$), but lower hysteresis (0.60% FSO) and higher sampling frequency (960 Hz, ~240 Hz with four channels) was purposed.[151] Fatigue effects have also been studied contributing to 0.25% FSO after over 10,000 pressure cycles. It was used to study IMP in anesthetized rabbits.[168]

2.3 *Intra-Articular Pressure*

Intra-articular pressure (IAP) is associated with joint and capsule loading.[169] It is a complex function of volume, time, joint angle, joint history, pathology, fluid distribution, and muscle action.[170] In the first study using FOS, IAP was monitored during continuous passive motion of the knee joint, a common post-surgery therapeutic procedure.[132] The FOS system consisted of a pressure transducer-tipped catheter (Camino Laboratories, San Diego, California) similar to those intended for intravascular and IMP measurements. Similar sensors were used to measure IAP in cadaveric glenohumeral joints[133] and during *in vivo* studies of the elbow joint in patients suffering from cubital tunnel syndrome.[134,135]

The potentialities of FBG for joint pressure mapping were explored by Mohanty et al.[27,171] A FBG array was developed to map stresses across the tibio-femoral interface during total knee arthroplasty. The array was embedded into a stack of unidirectional fiber-reinforced composite (PMMA) and molded to adapt to the femur condyles surface. Embedding is important to enhance FBG sensitivity to transverse loading.[27,57,172] Each OF was composed of sampled chirped FBG sensors capable of detecting force magnitude and its application point. *Ex vivo* experiments were carried out to sense prosthetic misalignments trough the analysis of contact stress distribution during knee flexion/extension.[27]

Dennison et al.[19,20,116] used minimally invasive FBG sensors to assess the pressure in the nucleus pulposus of intervertebral discs. It was recognized that large diameters of previously used nonoptical sensors (e.g., 1.5 mm OD)[173] could interfere with the normal behavior of the joint and induce degenerative effects.[173–175] Dennison's first proposal consisted of a bare FBG sensor (125 μm OD, 10 mm length, Bragg wavelength 1550 nm) that was left directly in contact with the nucleus pulposus.[116] After that, a configuration with increased spatial resolution and less affected by the inhomogeneity of the nucleus material was presented.[19,20] This new sensor was housed within a stainless-steel hypodermic tube allowing only just the tip to sense the external pressure. The sensing area, with 0.4 mm OD, consisted of exposed surfaces of silicone sealant (Dow Corning 3140 RTV, Midland, Michigan) and of the OF. Under pressure, the area was compressed inducing a shift in the Bragg wavelength. Sensor's mean sensitivity to pressure was $(-22.7 \pm 1.5\ \mathrm{E}^{-5})$ mV MPa^{-1}. Data from *ex vivo* porcine compression tests suggested a linear relation between intradiscal pressure and compressive load (mean coefficient of determination, $r^2 = 0.97$). A good agreement was obtained with SG sensors. Yet the mean relative difference in disc response to load between the FBG sensors and the SG sensor was 9.39% and ranged from 0.424% to 33.2%.[20] Dennison et al.[19] compared the sensor's sensitivity obtained from strain-optic relationships used in finite element analysis (FEA) with that obtained from experimental results. FEA sensitivity was -23.9 pm MPa^{-1} ($r^2 = 1$) and experimental sensitivity was -21.5 ± 0.07 pm MPa^{-1} ($r^2 = 0.99$). Using experimental sensitivity as reference the relative difference between these sensitivities was 11.1%.[19]

The above FBG sensors have not been tested *in vivo* and will require further efforts to be available as commercial plug-and-play devices. Meanwhile, F-P sensors from Samba Sensors (Västra Frölunda, Sweden) and Radi Medical Systems (Uppsala, Sweden) are already available to measure intradiscal pressure. Samba Preclin 360 transducer is a micromachined silicon sensor (photolithographic and wet etching techniques were applied) with 0.36 mm OD and a pressure range from −0.1 to 17 bar.[176] Depending on the pressure range its accuracy is of ±20 mbar and ±2.5% of reading (from −0.1 to 10 bar) or ±20 mbar and ±3% of reading (from 10 to 17 bar).[176]

Temperature coefficient is less than 14 mbar °C^{-1} for a temperature range between 20°C and 45°C.[176] Additionally, it can be coated with radiopaque material to be used in x-ray studies.[176] Some studies reported its use in pigs,[177,178] rabbits,[179] and human cadaveric spines.[180] In the case of the Radi Medical Systems sensor, it was used to monitor intradiscal pressure in sedated pigs[181] and patients suffering from lumbar back pain.[182] With 0.55-mm OD this sensor exhibits a pressure range from 0 to 800 kPa, a combined nonlinearity and hysteresis of <0.5% FSO, and a time response of less than 0.2 s.[182] Despite their small size, these sensors can still damage intervertebral discs; namely, those from small animals (e.g., rats). Meanwhile, Hsieh et al.[183] and Nesson et al.[18,184] were encouraged to overcome this limitation. They presented a low-coherence interferometric-based optical interrogation system with a sensor probe of 366 μm OD. The glass tube F-P cavity (15.2 μm length) was composed of two mirrors, a biocompatible polymer-metal composite diaphragm, and a well-cleaved end face of a SMF. It was fabricated by simple batch-fabrication methods without necessity of a cleanroom environment. The sensor exhibited a linear response to the applied pressure over the range of 0 to 70 kPa, a sensitivity of 0.0206 μm kPa^{-1} and a resolution of 0.17 kPa. Despite being attractive for *in vivo* and clinical practice, due to its biocompatible diaphragm and small size, it was used only for *in vitro* measurements of rodent tail discs.[18,183–185]

2.4 *Intracranial Pressure*

ICP is the pressure inside the skull; namely, in the brain tissue and cerebrospinal fluid. Following the original works of Adson and Lillie,[78] Guillaume and Janny,[81] and Lundberg,[82] continuous monitoring of ICP became a routine method in neurosurgery. Depending on the location of the sensor inside the skull the techniques to measure ICP may be classified as intraventricular, subdural/subarachnoid, or epidural technique.[186] The intraventricular catheter is placed directly at the ventricle and allows the most accurate ICP measurements.[186] However, this deep location in the brain also presents the highest risk of infection.[106,187] The subarachnoid catheter projects through the Dura into the subarachnoid space.[186,188] The epidural technique is the less invasive as it avoids introduction of the catheter through the brain parenchyma restricting the risk of infection to the extradural space.[187] Unfortunately, with this technique ICP results are usually overestimated, making it not recommended for neurocritical care patients.[189,190] The technique is useful in patients requiring ICP monitoring for long periods (>5 days) because in these patients the most important information is provided by analysis of the frequency and amplitude of slow ICP waves.[190]

First ICP measurements[136,191,192] resulted from the adaptation of the intravascular Camino sensor (Camino Laboratories, San Diego, California) originally proposed by Lekholm and Lindström.[40,45] Camino model 110-4B was considered to be accurate and reliable for ICP monitoring, presenting high-quality readings under laboratory and clinical conditions, a good correlation with SG sensors and fluid-filled systems, less drift and improved waveform resolution, insensitivity to hydrostatic artifacts and no flushing or infusion requirements.[101,102,104,112,193,194] On the other hand, they also underwent extensive scrutiny leading to identification of several drawbacks and questioning their routine use, particularly in clinical practice. Transducer failures (e.g., breakage, cable kinking, probe dislocation, abnormal readings, etc.) may range from 10% to 25%.[107] In the study of Yablon et al.,[102] 12% of sensors failures were caused by breakage of its components. Moreover, contamination of the probes is frequent and long-term monitoring seems to be associated with higher rates of infection.[106] Yet clinically significant infections were considered to be rare.[106] To minimize infections and zero drift of the transducer the manufacturer recommends placement of a new system under sterile conditions if monitoring is continued for more than five days.[99] Several studies have addressed the drift characteristics of the transducer either in laboratory[104] or clinical practice.[101,106,107] Zero drift is an important feature because this type of transducers cannot be re-zeroed after implantation, meaning that cumulative significant errors may occur in long-term monitoring.[101,106] Electrical calibration of external monitors is possible, but it cannot correct for inherent zero drift of the catheter once it is implanted.[107] Manufacturers' specifications for model 110-4B indicate a maximum zero drift during the first 24 h from 0 to ±2 mmHg and less than ±1 mmHg day^{-1} on subsequent days.[99] Thus a continuous five-day monitoring can introduce a maximum error of 6 mmHg. This is not satisfactory because normal values for ICP usually range from 7 to 15 mmHg in adults and from 3 to 7 mmHg in children.[109] Furthermore, values exceeding 20 mmHg require immediate treatment.[195] Laboratory tests have indicated the transducer complied with manufacturers' zero drift specifications, while results from clinical practice have suggested zero drift can be greater than reference values. As an example, Crutchfield et al.[101] found a larger maximum daily drift of ±2.5 mmHg, a lesser average daily drift of ±0.6 mmHg and an average drift over a five-day period of ±2.1 mmHg. Münch et al.[105] reported an average daily drift within reference values but after being removed from the patient it was 3.2± 17.2 mmHg for 50% of the probes. This value was normalized to the number of days of monitoring and decreased to only 6%.[105] Martinez-Manas et al.[106] reported only six of 56 implanted probes exhibited no zero drift, while the other readings ranged from a minimum of −24 mmHg and a maximum of +35 mmHg. After comparing their results with manufacturer's specifications, they conclude that 61% of the probes performed according to the expected values. It is interesting to note that no correlation was found between zero drift and the duration of monitoring.[106,107] Sensitivity to temperature remains a problem. A maximum of 3 mmHg over a temperature range of 22°C to 38°C is reported by the manufacturer.[99] However, in the study of Czosnyka et al.[104] temperature drift was ∼0.3 mmHg °C^{-1} leading to a maximum of 4.8 mmHg for the same temperature range.

The insertion method of 110-4B Camino transducer requires a drill hole through the skull of 2.71 mm OD.[99] Thus innovation with FOS may arrive from smaller sensors and less invasive procedures. Some recommendations were provided to those interested in developing new sensors for this purpose. According to Mignani and Baldini,[71] new sensors should meet a working range from −50 to 300 mmHg, a sensitivity of at least 0.1 mmHg, an accuracy of at least 1%, and a flat frequency response up to 1 kHz. The American National Standard for ICP monitoring, published by the AAMI,[196,197] includes minimum performance requirements that are clearly less demanding than those of Mignani and Baldini.[71] Pressure should range between 1 and 100 mmHg, the accuracy of ±2 mmHg in the range of 0 to 20 mmHg, and maximum error of 10% in the range of 20 to 100 mmHg.[196]

A good example of innovation effort was accomplished by Dennison and Wild[60] They developed an FBG sensor with 200 μm OD, a sensitivity of 58.7 pm MPa^{-1} and a sensing area of only 0.02 mm^2. Calibration results have demonstrated its ability to measure pressure with $\pm$2.7 mmHg repeatability over a range of 105 mmHg. This FBG sensor was proposed for ICP and blood-pressure measurements but is far away from clinical applications because *ex vivo* and *in vivo* tests are still to be done.

It is interesting to note that commercially available FOS are becoming competitive with each other. The Ventrix® ICP monitoring catheter (Integra LifeSciences, Plainsboro, New Jersey), the OPX100 transducer (InnerSpace, Tustin, California), the FOP-MIV (FISO Technologies, Québec, Canada) and the OPP-M series (OPP-M250 and OPP-M400; Opsens, Québec, Canada) pressure sensors are some possible candidates to compete with the most popular ICP Camino 110-4B transducer. The Ventrix® ICP monitoring catheter and the Camino 110-4B are from the same company, but the F-P OPX100 transducer is not and claims for new features, such as *in situ* re-zeroing and multimodal monitoring. In a comparative study the OPX-100 transducer presented a lower 24-h zero drift and temperature drift than the Camino 110-4B transducer.[104] On the other hand, the OPX-100 exhibited a static error (<8 mmHg) higher than that of 110-4B (<0.3 mm Hg). Furthermore, its bandwidth is lower (20 Hz) than that of 110-4B (33 to 120 Hz),[104] and it presents a high incidence (17%) of hematoma formation.[198] Few clinical data is available about this sensor and, to our best knowledge, it is no longer available. The FOP-MIV sensor is a versatile micro-optical mechanical system (MOMS) that can be used for many physiologic pressure measurements. It consists of a F-P vacuum cavity made of a micromachined silicon diaphragm membrane that is bonded on a cup-shaped glass base (550 μm OD). The F-P cavity is connected to a MMF and interrogated with white light.[142,144] According to manufacturers' specifications, FOP-MIV exhibits a measurement range from −300 to 300 mmHg, an accuracy equal to 1.5% FSO (or $\pm$1 mmHg), a resolution better than 0.3 mmHg, a thermal effect sensitivity of $-0.05\%\,°C^{-1}$ and a zero drift thermal effect of -0.4 mmHg $°C^{-1}$ (Ref. 21). The sensor allows for absolute external pressure measurements because vacuum inside cavity prevents pressure errors caused by gas thermal expansion.[142] Manufacturing technologies derived from the semiconductor industry (e.g., photolithography processes and automated assembly) allow their production in large quantities for a competitive price.[142] For ICP measurements the FOP-MIV can be introduced into catheters with diameters smaller than 1.2 mm.[142] However, to our best knowledge, ICP measurements with the FOP-MIV were made only in rats.[144,145] Both OPP-M250 (0.25 mm OD) and OPP-M400 (0.40 mm OD) have similar specifications (−50 to +300 mmHg pressure range; $\pm$1 mmHg precision; 0.2 mmHg accuracy; 4000 mmHg proof pressure; 10°C to 50°C operating temperature; 0% to 100% operating humidity range). They were specifically designed for physiological pressure measurements in preclinical environment and for OEM integration.[199] Besides ICP other possible applications of these F-P sensors include intra-vascular blood pressure, urodynamic pressure, intra-uterine pressure, intraocular pressure, and IAB pump therapy.[199] Nevertheless, almost all applications need to be supported by scientific publications.

2.5 *Other Pressure Applications*

Previously mentioned applications are probably the most common. Nevertheless, more contributions can be found concerning the use of FOS to sense pressure in other sites of the human body, such as the trachea,[200,201] the gastrointestinal tract,[2,56,202] and the intravaginal,[17] intraocular,[146] and intramedullary spaces.[147] We will explore some of them in the following lines.

Respiratory monitoring in paediatric or neonatal intensive care requires minimally invasive sensors for direct measurements of tracheal pressure. This was achieved for the first time using the Samba Resp. 420 transducer (Samba Sensors, Västra Frölunda, Sweden).[200,201] This F-P sensor has an OD of 420 μm contrasting with larger FOS, such as the Camino XP400 (1mm OD) (Camino Laboratories, San Diego, California), that have been used only in adults patients.[203] Samba Resp. 420 transducer is also a certified CE class IIb medical device approved for use in human patients within the European Union.[204] It exhibits a measurement range from -50 to $+350$ cmH_2O, an accuracy of $\pm$2.5% of reading (between -50 and $+250$ cmH_2O) or $\pm$4% of reading (between $+250$ to $+350$ cmH_2O), a temperature drift less than 0.2 $cmH_2O\,°C^{-1}$ (between 20°C and 45°C) and a response time of 1.3 ms.[200,204]

The possibility of measuring peristalsis (i.e., the rhythmic contraction of smooth muscles through the digestive tract) can help diagnosis of several gastrointestinal motility disorders. While this is possible using manometric techniques, particularly high-resolution solid-state and water-perfusion pressure sensors, the ability to present smaller, flexible and higher spatial resolution sensors remains a challenge. For example, an increase in the number of solid-state or water perfusion sensors into the same catheter is followed by increased complexity in signal processing, less flexibility, and larger catheter diameter.[2] For that reason the number of sensors per catheter is limited to ~36 for the solid-state technology and ~20 for the water perfused technology.[2] Such limitations can be overcome by exploring the potentialities of real time WDM to interrogate several inline FBG. In fact, this feature was accomplished by Arkwright et al.[56] using 32 inline FBG sensors (written between 815 and 850 nm; 3 mm length; 10 mm spaced) to measure the pressure along the esophagus of a subject.[2] To sense pressure each FBG was fixed to a rigid metallic substrate and a flexible diaphragm. Afterward, the multiplexed FBG array was inserted into a catheter of silicone rubber (3 mm OD), which was sealed at one of the extremities and the other connected to the data acquisition system. The excellent and significant correlation ($r \geq 0.992$) between the FBG based catheter and a reference solid-state catheter (Gaeltec, Dunvegan, Scotland; www.gaeltec.com) suggested one could substitute the other. Meanwhile, further studies have been published confirming FBG potentialities as multipoint or multiparameter sensors,[202,205] and their ability to incorporate new features, such as the measurement of longitudinal and circumferential muscular activity in the gastrointestinal tract.[202]

An interesting example of the versatility and applicability of FBG sensors was given by Ferreira et al.[17] who proposed a complete system for dynamic evaluation of the women pelvic floor muscle strength. The lack of muscle action seems to play an important role in development of several pelvic dysfunctions, such as urinary incontinence and genital prolapses. The system consisted of a silicone ergonomic intravaginal probe (100 mm length and 25 mm OD) with two inline FBG sensors and an

autonomous optoelectronic measurement unit. One FBG transduced radial muscle pressure into axial load, the other used for temperature referentiation. A mean sensitivity of ~120 pm N^{-1} was calculated for a measurement range of ~20 N. With temperature compensation, maximum estimated error (0.0075 N $°C^{-1}$) was considered negligible. Additionally, clinical trials were conducted in patients with pelvic floor disorders. Further improvements will include the substitution of silicone to eliminate some hysteretic behavior due to material's viscoelasticity and reduction of cross-sensitivity to axial induced load, torsion and bending.[17]

The possibility of using FOS to construct pressure-mapping devices to be placed in-between the body parts and supporting surfaces (e.g., floor, seat, mattress, cushion and backrest) is an exciting opportunity to enlarge the spectrum of FOS applications; namely, in the fields of medicine and rehabilitation, sports, ergonomics, automotive industry, etc. However, to accomplish it, FOS systems should compete with many recognized companies, such as Tekscan Inc. (South Boston, Massachusetts; www.tekscan.com) and Novel GmbH (Munich, Germany; http://novel.de) that are offering powerful accurate electronic-based systems at relatively low cost. Nevertheless, some limitations can be pointed to the above-mentioned technology. Tekscan sensors are based in conductive elastomers, which may exhibit nonlinear response, hysteresis, and gradual voltage drift.[206] Novel uses capacitive-based transducers, which can be affected by electrical interference and suffer from low spatial resolution, drift, and high sensitivity to temperature.[206] Moreover, with both technologies only normal loads and pressures can be measured. Thus, a window of opportunity is open to FOS capable of overcoming these limitations and introducing new features, namely the ability to measure normal and shear loads. A possible configuration was explored by Pleros et al.[12] by embedding multiplexed FBG arrays into PDMS silicon-polymer to built a pressure mat made of smaller scale blocks, each block consisting of four FBG sensors distributed to form a 2×2 matrix array with a square sensing area of 400 mm^2 and 25 mm thickness. Authors were also engaged in the FP7 project Intelligent Adaptable Surface with Optical Fiber Sensing for Pressure-Tension Relief (IASIS) that finished in 2011.[207] The IASIS project aimed to present intelligent rehabilitation systems based on multiplexed FBG arrays capable of sensing pressure in therapy beds or wheelchair seats and providing feedback information to prevent onset and evolution of pressure ulcers.[208] Same concept was extended to knee-socket interfaces to sense pressure in amputees.[209,210]

The possibility of using FOS to create smart systems and provide feedback about a patient's condition was also explored by Hao et al.[211] Bed surface mounted FBG arrays were proposed to monitor several clinical signals; namely, body pressure, respiratory rate, heart rate, and body temperature. Security alerts to prevent patients from maintaining prolonged static positions or falling out of the bed were also addressed. Sensor consisted of 12 inline FBG sensors (5 mm length each) organized to form a 3×4 matrix array that was mounted beneath the mattress surface of the bed. To sense pressure, each FBG was previously embedded into an arc-shaped elastic bending beam (40 mm length, 0.625 mm thick, and 2.2 mm height) using uneven layers of carbon fiber reinforced plastic. Calibration results suggested an excellent coefficient of determination ($r^2 = 0.9985$) between the wavelength shift and the applied load. Sensitivity obtained from the linear regression equation of calibrated data was equal to 0.1121 nm N^{-1}. Authors failed to present the algorithms used for pressure calculation. Vital signs, such as the respiratory rate and hearth rate, were assessed by signal processing techniques. Temperature sensor consisted of a FBG (10 mm length) isolated from strain by insertion into a glass/copper tube, which ends were encapsulated with a resin/epoxy system.[211]

Pressure mats are often used in biomechanical studies; namely, to analyze foot pressure distribution in static postures or dynamic activities, such as gait, jumping, running, or load carrying. This assessment has particular importance in diabetic insensitive feet because excessive pressure can lead to their ulceration, necrosis, and subsequent amputation.[212] The pedobarograph was probably the first device using optical techniques applied in clinical practice to study foot conditions. The upper glass surface of a pedobarograph is covered with a thin opaque material, usually a plastic sheet, which in contact with the feet changes the refractive index.[213,214] This action leads to light attenuation in the glass plate, making it possible to obtain a footprint and to calculate the applied pressure by means of light-intensity variation.[215] More recently, OF and FBG sensors were also introduced to sense foot pressure.[57,216] Multiplexed FBG arrays were positioned accordingly to the foot anatomy, embedded into uneven layers of carbon/epoxy laminates and cut into a shape of a footpad.[216] Calibration results suggested an excellent linear relationship ($r = 0.99927$) between the applied perpendicular load and wavelength shift. Wavelength sensitivity to load and pressure was ~5.44 pm N^{-1} and ~700 pm MPa^{-1}, respectively. A clinical experiment was conducted to evaluate pressure distribution under normal and abnormal standing.[216]

The study of Wang et al.[217] is of particular interest because it represents the first attempt to create in-shoe shear sensors. Instead of using a wavelength modulation design, sensor development was based on bend-loss technique. A 2×2 array of MMF, embedded into high-compliance material and forming four orthogonal intersection points (each with a sensing area of 100 mm^2), was used as a basic sensing sheet. Under compressive loading, light attenuation caused by physical deformation of the fibers at the intersection points was used to calculate the x and y coordinates of the pressure point and the corresponding normal stress. To obtain shear stress, two layers of the basic sensing sheet, placed between gel/polymeric shoe insole pads, were used. This way, the relative difference between the corresponding pressure points could be used to calculate the amount of shear. The entire system consisted of a LED source, an eight-element photodetector array, and a data-acquisition system (National Instrument 16-input, 500 kb s^{-1}, 12-bit multifunction input/output data-acquisition card; Lab-VIEW software; and a laptop computer). Repeatable results were obtained under bench mechanical loading tests consisting of vertical forces up to 6.5 N and displacements of 6 mm, and shear forces up to 13.8 N. The minimum detectable vertical and shear forces were 0.4 and 2.2 N (at 60 pitch angle), respectively. To address some limitations of the previous configuration (e.g., low spatial resolution, consistent and accurate manufacturing of the sensor, cost and noise) a batch process to fabricate PDMS-based waveguide sensor, and a neural network technique to provide an accurate description of the force distribution, were proposed in further studies.[206,218,219] After successful bench tests, the same group has recently presented a full-scale foot pressure/shear sensor, capable of measuring normal forces ranging from 19.09 to 1000 kPa.[220]

Table 2 Summary of the characteristics of the most representative fiber-optic pressure sensors.

Years	Sensor head	Modulation	Frequency response/ sampling rate	Sensitivity and linearity	Resolution	Accuracy	Working range	Temperature dependence	Hysteresis	Response time	Time Drift	Applications	References
1969/ 1970	ϕ 0.85 mm ϕ 1.5 mm	Intensity	dc to >15 kHz	2.5% FSO	—	0.5%c FSO	−50 to +200 mmHg	Insignificant 0 drift (20°C to 37°C)	Insignificant	~40 s	2.5 $mmHgh^{-1}$	Intravascular; *in vivo* blood pressure; dog and man	[40, 45]
1978	ϕ 1.5 mm	Intensity	1000 Hz	Up to 200 mmHg	—	4 to 5 mm H_2O	300 mmHg	0.44 mm $Hg°C^{-1}$	—	—	—	Intravascular/ intracardiac; *in vivo*; dog	[124]
1987/ 1991	300 × 300 ×275 μm	F-P	Up to 1000 Hz	2% of reading linearity ±2% of reading (−50 to 300 mmHg)	<1 mmHg	±1 mmHg	500 to 1100 mmHg	Insignificant	Nonlinearit $y < 0.1\%$	<1 msec	Offset drift 0.6± 0.03 mmHg over 2 h	Intravascular; left heart chamber and systemic arterial pressures; dog and goat	[88, 138, 139]
2011	ϕ 5.7 mm	F-P	—	1 mmHg (fringe counting); <0.1 mmHg (interpolation)	1 mmHg	10.5 mmHg	Up to 100 mmHg	0.15 mm $Hg°C^{-1}$	—	1 to 2 ms	—	Intravascular blood pressure; left ventricular pressure; *in vitro*	[141]
2005	ϕ 550 μm	F-P	250 Hz to 1 kHz	—	<0.3 mmHg	1.5% (±1 mmHg) of FSO	−300 to 300 mmHg	Thermal effect sensitivity 0.05%$°C^{-1}$ Zero drift thermal effect 0.4 mm $Hg°C^{-1}$	—	—	—	Left ventricular pressure; intracranial, intraocular; intramedullary pressure, pharyngeal pressure; animal and human	[21, 122, 142–147]
2003	ϕ 125 μm	F-P	—	−0.25 nm $mmHg^{-1}$	4 mmHg	—	−100 to 400 mmHg	Observed	—	—	—	Intravascular; goat	[115, 152]
2009	ϕ 125 μm	F-P	—	~550 nm bar^{-1} ~1100 nm bar^{-1}	300 Pa	—	Linear up to 0.4 bar (Max 78 bar) Non linear (max. 100 bar)	0.3 and 0.4 nm$°C^{-1}$	Zero-point shift (<2 nm) Zero-point shift (5 to 9 nm)	—	—	Intravascular; still to apply	[155]
2005	ϕ 125 μm	F-P	—	~0.63 rad kPa^{-1} (1550 nm) 2.1 mrad kPa^{-1}	10 Pa 600 Pa	—	0 to 40 kPa 0 to 1200 KPa	—	—	7 to 80 ms <3 ms	—	Intravascular; still to apply	[154]
2008	ϕ 125 μm	F-P	—	—	<0.4 mmHg	±5 mmHg ±8 mmHg	−25 to 125 mmHg −300 to 300 mmHg	Thermal effect sensitivity 0.1%$°C^{-1}$ Zero drift thermal effect 0.4 mmHg $°C^{-1}$	—	—	—	Intravascular; still to apply	[156, 157]

Table 2 (*Continued*).

Years	Sensor head	Modulation	Frequency response/ sampling rate	Sensitivity and linearity	Resolution	Accuracy	Working range	Temperature dependence	Hysteresis	Response time	Time Drift	Applications	References
1977	ϕ 2.1 mm	Intensity	—	—	—	—	0 to 250 mmHg	~0.3 mmHg°C^{-1}	—	—	1.25 mmHg h^{-1} 0 to ±2 mmHg/ 24 h <1 mmHg day^{-1}	Intravascular, intramuscular, intra-articular, intracranial; *in vivo* animal and human	[89, 94, 95, 101, 102, 104–107, 112, 89–136, 160, 161, 191–194]
2003 2009	ϕ 360 μm ϕ 250 to 280 μm	F-P	66 Hz (~10 Hz; 8 channels) 960 Hz (240 Hz; 4 channels)	1.6% FSO (8.78 mV mmHg^{-1}) 3.7 to 4.0 nm mmHg^{-1}	0.25 mmHg	1.5% FSO 1.8% FSO	0 to 250 mmHg	—	4.5% FSO 0.60% FSO	130 ms	—	Intramuscular; *in vivo*; animal	[93, 151, 165–168]
2007	—	FBG	—	120 pm MPa^{-1}	8 kPa	0.125 MPa	>5 MPa	—	—	—	—	Intra-articular (*ex vivo*)	[27, 171]
2008	ϕ 125 μm ϕ 0.4 mm	FBG	—	5.7± 0.085 pm MPa^{-1} −21.5± 0.07 pm MPa^{-1}	—	—	0 to 2 MPa	—	2.13% FSO 2.24% FSO	—	—	Intra-articular (*ex-vivo*)	[19–20, 116]
1999	ϕ 360 μm	F-P	—	—	—	±20 mbar and ±2.5% of reading ±20 mbar and ±3% of reading	−0.1 to 10 bar 10 to 17 bar	14 mbar °C^{-1}	—	—	—	Intra-articular; *in vivo* animal; *ex vivo* human	[176–180]
1994	ϕ 0.55 mm	F-P	5 Hz	—	—	—	0 to 800 kPa	—	<0.5% FSO	<200 ms	—	Intra-articular; animal and human	[181–182]
2006	ϕ 366 μm	F-P	—	0.0206 μm kPa^{-1}	0.17 kPa	—	0 to 70 kPa	—	—	—	—	Intra-articular; *in vitro* animal	[18, 183–185]
2008	ϕ 200 μm	FBG	1 Hz	58.7 pm MPa^{-1}	—	±2.7 mmHg	0 to 105 mmHg	—	—	—	—	Intracranial and blood pressure; still to apply	[60]
2011	ϕ 0.25 mm ϕ 0.40 mm	F-P	—	—	0.5 mmHg 0.2 mmHg	±0.2 mmHg	−50 to +300 mmHg	0.3 mmHg °C^{-1} 0.15 mmHg °C^{-1}	—	—	<3 mmHg/ 28 days <4 mmHg/ 28 days	Intracranial; intravascular; intraocular; still to apply	[199]
2001	ϕ 420 μm	F-P	—	—	—	±2.5% of reading ±4% of reading	−50 to +250 cmH_2O 250 to +350 cmH_2O	<0.2 cmH_2O °C^{-1}	—	1.3 ms	—	tracheal pressure	[200–201, 204]
2006	ϕ 25 mm	FBG	—	~120 pm N^{-1}	—	—	~20 N	0.0075 N °C^{-1}	—	—	—	women pelvic floor muscle strength	[17]
2001	—	FBG	—	~700 pm MPa^{-1}	3885.6 Nm^{-2}	—	0 to 4.66 ×10^5 Nm^{-2}	~13 pm °C^{-1}	—	—	—	Foot pressure	[57, 216]

In Table 2 a summary of the characteristics of the most representative FOS intended for pressure measurement is presented.

3 Final Remarks

The state of the art of FOS intended for pressure biomedical and biomechanics applications has been reviewed. Our approach to FOS was made after introducing conventional sensors and pointing out some of their limitations. FOS seems particularly suitable for use in minimally invasive procedures, allowing precise and accurate point, multipoint, or distributed measurements without the necessity of increasing sensor's dimensions and with easier instrumentation. Minimum dimensions are achieved when the OF itself is used as the sensing element, such as with FBG sensors and all-fused-silica designs. Nevertheless, small dimensions are also related to mechanical fragility. FOS without protective layers require special handling. They can be suitable for *in vitro* or *ex vivo* biomechanical experiments, but will fail during *in vivo* trials and clinical practice. Thus, the use of biocompatible and sterilizable layers, capable of maintaining the minimally invasive function and provide mechanical stability, is mandatory.

FOS technology has about 40 years of history and most underlying working principles are sufficiently mature to provide accurate solutions for sensing almost any physical and chemical quantity. Despite that, few companies are exploring FOS potential and offering turnkey solutions for biomedical and biomechanical sensing. Even fewer have supported their products with peer-reviewed papers, standardized testing protocols, or approvals from regulatory/standardization entities. These are, indeed, the greatest challenges for those wishing to develop FOS for biomechanical and biomedical applications, especially for the medical market.

Acknowledgments

This work was supported by the Portuguese Foundation for Science and Technology (FCT) fellowship SFRH/BD/45130/2008.

References

1. A. G. Mignani and F. Baldini, "Biomedical sensors using optical fibres," *Rep. Prog. Phys.* **59**(1), 1–28 (1996).
2. J. W. Arkwright et al., "*In-vivo* demonstration of a high resolution optical fiber manometry catheter for diagnosis of gastrointestinal motility disorders," *Opt. Express* **17**(6), 4500–4508 (2009).
3. M. E. Ladd and H. H. Quick, "Reduction of resonant RF heating in intravascular catheters using coaxial chokes," *Magn. Reson. Med.* **43**(4), 615–619 (2000).
4. G. Voskerician et al., "Biocompatibility and biofouling of MEMS drug delivery devices," *Biomaterials* **24**(11), 1959–1967 (2003).
5. D. J. Monk et al., "Determination of the etching kinetics for the hydrofluoric acid/silicon dioxide system," *J. Electrochem. Soc.* **140**(8), 2339–2346 (1993).
6. J. Bühler et al., "Silicon dioxide sacrificial layer etching in surface micromachining," *J. Micromech. Microeng.* **7**(1), R1–R13 (1997).
7. M. Thompson and E. T. Vandenberg, "*In vivo* probes: problems and perspectives," *Clin. Biochem.* **19**(5), 255–261 (1986).
8. D. R. Biswas, "Characterization of polyimide-coated optical fibers," *Opt. Eng.* **30**(6), 772–775 (1991).
9. D. R. Biswas, "Optical fiber coatings for biomedical applications," *Opt. Eng.* **31**(7), 1400–1403 (1992).
10. E. Samset et al., "Temperature measurement in soft tissue using a distributed fibre Bragg-grating sensor system," *Minim. Invasiv. Ther.* **10**(2), 89–93 (2001).
11. L. Chen et al., "Study of laser ablation in the *in vivo* rabbit brain with MR thermometry," *J. Magn. Reson. Imag.* **16**(2), 147–152 (2002).
12. N. Pleros et al., "Optical fiber sensors in orthopedic biomechanics and rehabilitation," in *9th Int. Conf. Information Technology Applications Biomedicine (ITAB)*, pp. 1–4, IEEE, Larnaca, Cyprus (2009).
13. U. Wonneberger et al., "Intradiscal temperature monitoring using double gradient-echo pulse sequences at 1.0T," *J. Magn. Reson. Imag.* **31**(6), 1499–1503 (2010).
14. A. A. Stolov et al., "Thermal stability of specialty optical fibers," *J. Lightwave Technol.* **26**(20), 3443–3451 (2008).
15. D. J. Webb et al., "First *in-vivo* trials of a fiber Bragg grating based temperature profiling system," *J. Biomed. Opt.* **5**(1), 45–50 (2000).
16. U. Utzinger and R. R. Richards-Kortum, "Fiber optic probes for biomedical optical spectroscopy," *J. Biomed. Opt.* **8**(1), 121–147 (2003).
17. L. A. Ferreira et al., "Dynamic assessment of women pelvic floor function by using a fiber Bragg grating sensor system," *Proc. SPIE* **6083**, H1–H10 (2006).
18. S. Nesson et al., "Miniature fiber optic pressure sensor with composite polymer-metal diaphragm for intradiscal pressure measurements," *J. Biomed. Opt.* **13**(4), 044040 (2008).
19. C. R. Dennison et al., "A minimally invasive in-fiber Bragg grating sensor for intervertebral disc pressure measurements," *Meas. Sci. Technol.* **19**(8), 1–12 (2008).
20. C. R. Dennison et al., "Validation of a novel minimally invasive intervertebral disc pressure sensor utilizing in-fiber Bragg gratings in a porcine model: an *ex vivo* study," *Spine* **33**(17), E589–E594 (2008).
21. FISO, "FOP-MIV product datasheet," http://www.fiso.com/admin/useruploads/files/fop-miv.pdf (10 May 2013).
22. J. Xu, "High temperature high bandwidth fiber optic pressure sensors," Ph.D. Thesis, State University (2005).
23. E. Udd, *Fiber Optic Sensors: An Introduction For Engineers And Scientists*, Wiley Interscience, New York (1991).
24. G. Wehrle et al., "A fibre optic Bragg grating strain sensor for monitoring ventilatory movements," *Meas. Sci. Technol.* **12**(7), 805–809 (2001).
25. D. A. Jackson and J. D. C. Jones, "Fibre optic sensors," *Opt. Acta Int. J. Opt.* **33**(12), 1469–1503 (1986).
26. T. Fresvig et al., "Fibre optic Bragg grating sensors: an alternative method to strain gauges for measuring deformation in bone," *Med. Eng. Phys.* **30**(1), 104–108 (2008).
27. L. Mohanty et al., "Fiber grating sensor for pressure mapping during total knee arthroplasty," *Sensor Actuat. A Phys.* **135**(2), 323–328 (2007).
28. H. H. Hopkins and N. S. Kapany, "A flexible fibrescope using static scanning," *Nature* **173**(4392), 39–41 (1954).
29. M. L. Polanyi and R. M. Hehir, "*In vivo* oximeter with fast dynamic response," *Rev. Sci. Instrum.* **33**(10), 1050–1054 (1962).
30. Y. Enson et al., "*In vivo* studies with an intravascular and intracardiac reflection oximeter," *J. Appl. Physiol.* **17**(3), 552–558 (1962).
31. Y. Enson et al., "Intracardiac oximetry in congenital heart disease," *Circulation* **29**, 499–507 (1964).
32. F. Clark et al., "Fiber optic blood pressure catheter with frequency response from DC into the audio range," in *Proc. Nat. Elec. Conf.*, McCormick Place, Chicago, IL (1965).
33. W. J. Gamble et al., "The use of fiberoptics in clinical cardiac catheterization: I. Intracardiac oximetry," *Circulation* **31**(3), 328–343 (1965).
34. P. G. Hugenholtz et al., "The use of fiberoptics in clinical cardiac catheterization: II. *In vivo* dye-dilution curves," *Circulation* **31**(3), 344–355 (1965).
35. P. L. Frommer et al., "Clinical applications of an improved, rapidly responding fiberoptic catheter," *Am. J. Cardiol.* **15**(5), 672–679 (1965).
36. D. C. Harrison et al., "Fiber optics for continuous *in vivo* monitoring of oxygen saturation," *Am. Heart J.* **71**(6), 766–774 (1966).
37. B. McCarthy et al., "Fiberoptic monitoring of cardiac output and hepatic dye clearance in dogs," *J. Appl. Physiol.* **23**(5), 641–645 (1967).
38. G. A. Mook et al., "Fibre optic reflection photometry on blood," *Cardiovasc. Res.* **2**(2), 199–209 (1968).
39. A. Ramirez et al., "Registration of intravascular pressure and sound by a fiberoptic catheter," *J. Appl. Physiol.* **26**(5), 679–683 (1969).
40. A. Lekholm and L. H. Lindström, "Optoelectronic transducer for intravascular measurements of pressure variations," *Med. Biol. Eng. Comput.* **7**(3), 333–335 (1969).
41. P. G. Hugenholtz et al., "Application of fiberoptic dye-dilution technic to the assessment of myocardial function. I. Description of technic and

results in 100 patients with congenital or acquired heart disease," *Am. J. Cardiol.* **24**(1), 79–94 (1969).
42. R. Singh et al., "Simultaneous determinations of cardiac output by thermal dilution, fiberoptic and dye-dilution methods," *Am. J. Cardiol.* **25**(5), 579–587 (1970).
43. S. Silvestri and E. Schena, "Optical-fiber measurement systems for medical applications," in *Optoelectronics: Devices and Applications*, P. Predeep, Ed., pp. 205–224, InTech, Rijeka, Croatia (2011).
44. P. Roriz et al., "Fiber optic intensity-modulated sensors: a review in biomechanics," *Photon. Sens.* **2**(4), 315–330 (2012).
45. L. H. Lindström, "Miniaturized pressure transducer intended for intravascular use," *IEEE Trans. Bio-Med. Eng.* **BME-17**(3), 207–219 (1970).
46. J. N. Fields et al., "Fiber optic pressure sensor," *J. Acoust. Soc. Am.* **67**(3), 816–818 (1980).
47. C. Fabry and A. Perot, *Mesure De Petites Epaisseurs En Valeur Absolue*, Academie des Sciences, Paris (1898).
48. F. T. S. Yu and Y. Shizhuo, Eds., *Fiber Optic Sensors*, Marcel Dekker Inc., New York (2002).
49. K. O. Hill et al., "Photosensitivity in optical fiber waveguides: application to reflection filter fabrication," *Appl. Phys. Lett.* **32**(10), 647–649 (1978).
50. K. O. Hill et al., "Photosensitivity in optical fibers," *Annu. Rev. Mater. Sci.* **23**(1), 125–157 (1993).
51. G. Meltz et al., "Formation of Bragg gratings in optical fibers by a transverse holographic method," *Opt. Lett.* **14**(15), 823–825 (1989).
52. D. B. Keck, *Optoelectronics in Japan and the United States*, Japanese Technology Evaluation Center (JTEC), Baltimore, MD (1996).
53. A. Othonos, "Fiber Bragg gratings," *Rev. Sci. Instrum.* **68**(12), 4309–4341 (1997).
54. Y. J. Rao and D. A. Jackson, "Recent progress in multiplexing techniques for in-fiber Bragg grating sensors," *Proc. SPIE* **2895**, 171–182 (1996).
55. Y. J. Rao et al., "Simultaneously spatial-time and wavelength-division-multiplexed in-fiber Bragg grating sensor network," *Proc. SPIE* **2838**, 23–30 (1996).
56. J. W. Arkwright et al., "The use of wavelength division multiplexed fiber Bragg grating sensors for distributed sensing of pressure in the gastrointestinal tract," in *IEEE Photonics Global Conf (IPGC)*, pp. 1–4, IEEE, Singapore (2008).
57. S. C. Tjin et al., "A pressure sensor using fiber Bragg grating," *Fiber Integrated Opt.* **20**(1), 59–69 (2001).
58. Y. J. Rao et al., "In-fiber Bragg-grating temperature sensor system for medical applications," *J. Lightwave Technol.* **15**(5), 779–785 (1997).
59. S. W. James et al., "Strain response of fibre Bragg grating sensors at cryogenic temperatures," *Meas. Sci. Technol.* **13**(10), 1535–1539 (2002).
60. C. R. Dennison and P. M. Wild, "Enhanced sensitivity of an in-fibre Bragg grating pressure sensor achieved through fibre diameter reduction," *Meas. Sci. Technol.* **19**(12), 1–11 (2008).
61. V. Mishra et al., "Fiber grating sensors in medicine: current and emerging applications," *Sensor Actuat. A Phys.* **167**(2), 279–290 (2011).
62. D. L. Polla et al., "Microdevices in medicine," *Annu. Rev. Biomed. Eng.* **2**(1), 551–576 (2000).
63. J. Voldman et al., "Microfabrication in biology and medicine," *Annu. Rev. Biomed. Eng.* **1**(1), 401–425 (1999).
64. R. Stendel et al., "Clinical evaluation of a new intracranial pressure monitoring device," *Acta Neurochir.* **145**(3), 185–193 (2003).
65. G. Citerio et al., "Bench test assessment of the new Raumedic Neurovent-P ICP sensor: a technical report by the BrainIT Group," *Acta Neurochir.* **146**(11), 1221–1226 (2004).
66. G. Citerio et al., "Multicenter clinical assessment of the Raumedic Neurovent-P Intracranial Pressure Sensor: a report by the BrainIt Group," *Neurosurgery* **63**(6), 1152–1158 (2008).
67. L. Wang and D. J. Beebe, "Shear sensitive silicon piezoresistive tactile sensor prototype," *Proc. SPIE* **3514**, 359–367 (1998).
68. J. Peterson and G. Vurek, "Fiber-optic sensors for biomedical applications," *Science* **224**(4645), 123–127 (1984).
69. M. Martin et al., "Fibre-optics and optical sensors in medicine," *Med. Biol. Eng. Comput.* **25**(6), 597–604 (1987).
70. D. R. Walt, "Fiber-optic sensors for continuous clinical monitoring," *Proc. IEEE* **80**(6), 903–911 (1992).
71. A. G. Mignani and F. Baldini, "*In-vivo* biomedical monitoring by fiber-optic systems," *J. Lightwave Technol.* **13**(7), 1396–1406 (1995).
72. A. Heller, "Implanted electrochemical glucose sensors for the management of diabetes," *Annu. Rev. Biomed. Eng.* **1**(1), 153–175 (1999).
73. O. S. Wolfbeis, "Fiber-optic chemical sensors and biosensors," *Anal. Chem.* **74**(12), 2663–2678 (2002).
74. B. Ravary et al., "Strain and force transducers used in human and veterinary tendon and ligament biomechanical studies," *Clin. Biomech.* **19**(5), 433–447 (2004).
75. M. Bosch et al., "Recent development in optical fiber biosensors," *Sensors* **7**(6), 797–859 (2007).
76. A. Leung et al., "A review of fiber-optic biosensors," *Sensor Actuat. B Chem.* **125**(2), 688–703 (2007).
77. S. E. Stitzel et al., "Artificial noses," *Annu. Rev. Biomed. Eng.* **13**(1), 1–25 (2011).
78. A. W. Adson and W. L. Lillie, "The relationship of intracerebral pressure, choked disc, and intraocular tension," *Trans. Am. Acad. Ophthalmol. Otolaryngol.* **30**, 138–154 (1927).
79. G. E. Burch and W. A. Sodeman, "The estimation of the subcutaneous tissue pressure by a direct method," *J. Clin. Invest.* **16**(6), 845–850 (1937).
80. O. H. Gauer and E. Gienapp, "A miniature pressure-recording device," *Science* **112**(2910), 404–405 (1950).
81. J. Guillaume and P. Janny, "Manométrie intra-crânienne continue: Intérêt pathophysiologique et clinique de la méthode," *Presse Med.* **59**, 953–955 (1951).
82. N. Lundberg, "Continuous recording and control of ventricular fluid pressure in neurosurgical practice," *Acta Psychiatr. Scand. Suppl.* **36**(149), 1–193 (1960).
83. A. Nachemson and J. M. Morris, "*In vivo* measurements of intradiscal pressure: discometry, a method for the determination of pressure in the lower lumbar discs," *J. Bone Joint Surg. Am.* **46**(5), 1077–1092 (1964).
84. A. Nachemson, "*In vivo* discometry in lumbar discs with irregular nucleograms: some differences in stress distribution between normal and moderately degenerated discs," *Acta Orthop.* **36**(4), 418–434 (1965).
85. P. F. Scholander et al., "Negative pressure in the interstitial fluid of animals," *Science* **161**(3839), 321–328 (1968).
86. S. L. Weinhoffer et al., "Intradiscal pressure measurements above an instrumented fusion: a cadaveric study," *Spine* **20**(5), 526–531 (1995).
87. T.-E. Hansen, "A fiberoptic micro-tip pressure transducer for medical applications," *Sensor Actuat.* **4**, 545–554 (1983).
88. R. A. Wolthuis et al., "Development of medical pressure and temperature sensors employing optical spectrum modulation," *IEEE Trans. Bio-Med. Eng.* **38**(10), 974–981 (1991).
89. A. G. Crenshaw et al., "A new transducer-tipped fiber optic catheter for measuring intramuscular pressures," *J. Orthop. Res.* **8**(3), 464–468 (1990).
90. S. Mubarak et al., "The wick catheter technique for measurement of intramuscular pressure. A new research and clinical tool," *J. Bone Joint Surg. Am.* **58**(7), 1016–1020 (1976).
91. C. H. Rorabeck et al., "Compartmental pressure measurements: an experimental investigation using the slit catheter," *J. Traum* **21**(6), 446–449 (1981).
92. B. J. Awbrey et al., "Chronic exercise-induced compartment pressure elevation measured with a miniaturized fluid pressure monitor," *Am. J. Sport Med.* **16**(6), 610–615 (1988).
93. K. R. Kaufman et al., "Performance characteristics of a pressure microsensor," *J. Biomech.* **36**(2), 283–287 (2003).
94. K. R. Kaufman and D. H. Sutherland, "Dynamic intramuscular pressure measurement during gait," *Oper. Tech. Sports Med.* **3**(4), 250–255 (1995).
95. A. G. Crenshaw et al., "Intramuscular pressures during exercise: an evaluation of a fiber optic transducer-tipped catheter system," *Eur. J. Appl. Physiol. Occup. Physiol.* **65**(2), 178–182 (1992).
96. M. Czosnyka et al., "Laboratory testing of the Spiegelberg brain pressure monitor: a technical report," *J. Neurol. Neurosurg. Psychiatr.* **63**(6), 732–735 (1997).
97. S. Morikawa, "Fiberoptic catheter-tip pressure transducer," *Jpn. J. Med. Electron. Biol. Eng.* **10**(1), 36–39 (1972).
98. K. Kobayashi et al., "Fiberoptic catheter-tip micromanometer," *Jpn. J. Med. Electron. Biol. Eng.* **15**(7), 465–472 (1977).
99. INTEGRA, "Directions for use: OLM intracranial pressure monitoring kit model 110-4B," http://integralife.com/products/PDFs/Camino/110-4B.pdf (10 May 2013).
100. P. Hollingsworth-Fridlund et al., "Use of fiber-optic pressure transducer for intracranial pressure measurements: a preliminary report," *Heart Lung* **17**(2), 111–120 (1988).

101. J. S. Crutchfield et al., "Evaluation of a fiberoptic intracranial pressure monitor," *J. Neurosurg.* **72**(3), 482–487 (1990).
102. J. Yablon et al., "Clinical experience with a fiberoptic intracranial pressure monitor," *J. Clin. Monitor Comput.* **9**(3), 171–175 (1993).
103. N. Bruder et al., "A comparison of extradural and intraparenchymatous intracranial pressures in head injured patients," *Intensive Care Med.* **21**(10), 850–852 (1995).
104. M. Czosnyka et al., "Laboratory testing of three intracranial pressure microtransducers: technical report," *Neurosurgery* **38**(1), 219–224 (1996).
105. E. Münch et al., "The CAMINO intracranial pressure device in clinical practice: reliability, handling characteristics and complications," *Acta Neurochir.* **140**(11), 1113–1120 (1998).
106. R. Martinez-Manas et al., "Camino® intracranial pressure monitor: prospective study of accuracy and complications," *J. Neurol. Neurosurg. Psychiatr.* **69**(1), 82–86 (2000).
107. I. Piper et al., "The Camino intracranial pressure sensor: is it optimal technology? An internal audit with a review of current intracranial pressure monitoring technologies," *Neurosurgery* **49**(5), 1158–1165 (2001).
108. M. Gelabert-Gonzalez et al., "The Camino intracranial pressure device in clinical practice. Assessment in a 1000 cases," *Acta Neurochir.* **148**(4), 435–441 (2006).
109. M. Smith, "Monitoring intracranial pressure in traumatic brain injury," *Anesth. Analg.* **106**(1), 240–248 (2008).
110. P. K. Eide, "Comparison of simultaneous continuous intracranial pressure (ICP) signals from ICP sensors placed within the brain parenchyma and the epidural space," *Med. Eng. Phys.* **30**(1), 34–40 (2008).
111. A. Bekar et al., "Risk factors and complications of intracranial pressure monitoring with a fiberoptic device," *J. Clin. Neurosci.* **16**(2), 236–240 (2009).
112. P. H. Raboel et al., "Intracranial pressure monitoring: invasive versus non-invasive methods: a review," *Crit. Care Res. Pract.* **2012**, 1–14 (2012).
113. E. Cox and B. Jones, "Fiber optic color sensors based on Fabry-Pérot interferometry," in *1st Int. Conf. Opt. Fiber Sensors*, Inspec/IEE, London, UK (1983).
114. E. W. Saaski et al., "A fiber-optic sensing system based on spectral modulation," in *Proc. ISA/86 Int. Conf. and Exhibition*, pp. 86–2803, ISA, Houston, TX (1986).
115. K. Totsu et al., "Ultra-miniature fiber-optic pressure sensor using white light interferometry," *J. Micromech. Microeng.* **15**(1), 71–75 (2005).
116. C. R. Dennison et al., "*Ex vivo* measurement of lumbar intervertebral disc pressure using fibre-Bragg gratings," *J. Biomech.* **41**(1), 221–225 (2008).
117. H. D. Dear and A. F. Spear, "Accurate method for measuring dP-dt with cardiac catheters and external transducers," *J. Appl. Physiol.* **30**(6), 897–899 (1971).
118. K. L. Gould et al., "*In vivo* comparison of catheter manometer systems with the catheter-tip micromanometer," *J. Appl. Physiol.* **34**(2), 263–267 (1973).
119. P. D. Stein et al., "Comparison of the distribution of intramyocardial pressure across the canine left ventricular wall in the beating heart during diastole and in the arrested heart. Evidence of epicardial muscle tone during diastole," *Circ. Res.* **47**(2), 258–267 (1980).
120. C. W. Yeomanson and D. H. Evans, "The frequency response of external transducer blood pressure measurement systems: a theoretical and experimental study," *Clin. Phys. Physiol. Meas.* **4**(4), 435–449 (1983).
121. J. P. J. Kroehle et al., "A thorough characterization of the frequency response of various *in vivo* blood pressure measurement technologies," in *Society of Toxicology, Annual Meeting*, Society of Toxicology, Washington, DC (2010).
122. E. Pinet et al., "Miniature fiber optic pressure sensor for medical applications: an opportunity for intra-aortic balloon pumping (IABP) therapy," *Proc. SPIE* **5855**, 234–237 (2005).
123. J. B. Taylor et al., "*In vivo* monitoring with a fiber optic catheter," *J. Am. Med. Assoc.* **221**(7), 667–673 (1972).
124. H. Matsumoto et al., "The development of a fibre optic catheter tip pressure transducer," *J. Med. Eng. Technol.* **2**(5), 239–242 (1978).
125. U. Ozerdem, "Measuring interstitial fluid pressure with fiberoptic pressure transducers," *Microvasc. Res.* **77**(2), 226–229 (2009).
126. P. Polygerinos et al., "Novel miniature MRI-compatible fiber-optic force sensor for cardiac catheterization procedures," in *IEEE Int. Conf. Robotics Automation (ICRA)*, pp. 2598–2603, IEEE, Anchorage, AK (2010).
127. L. Tenerz et al., "A fiberoptic silicon pressure microsensor for measurements in coronary arteries," in *IEEE Int. Conf. Solid-State Sensor Actuator*, pp. 1021–1023, IEEE, San Francisco, CA (1991).
128. O. Tohyama et al., "A fiber-optic silicon pressure sensor for ultra-thin catheters," *Sensor Actuat. A Phys.* **54**(1–3), 622–625 (1996).
129. C. Strandman et al., "A production process of silicon sensor elements for a fibre-optic pressure sensor," *Sensor Actuat. A Phys.* **63**(1), 69–74 (1997).
130. O. Tohyama et al., "A fiber-optic pressure microsensor for biomedical applications," *Sensor Actuat. A Phys.* **66**(1–3), 150–154 (1998).
131. E. Kalvesten et al., "The first surface micromachined pressure sensor for cardiovascular pressure measurements," in *The Eleventh Annual Int. Workshop on Micro Electro Mechanical Systems, 1998 (MEMS 98. Proc.)*, pp. 574–579, IEEE, Heidelberg, Germany (1998).
132. R. A. Pedowitz et al., "Intraarticular pressure during continuous passive motion of the human knee," *J. Orthop. Res.* **7**(4), 530–537 (1989).
133. W. Inokuchi et al., "The relation between the position of the glenohumeral joint and the intraarticular pressure: an experimental study," *J. Shoulder Elb. Surg.* **6**(2), 144–149 (1997).
134. K. Iba et al., "Intraoperative measurement of pressure adjacent to the ulnar nerve in patients with cubital tunnel syndrome," *J. Hand Surg. Am.* **31**(4), 553–558 (2006).
135. K. Iba et al., "The relationship between the pressure adjacent to the ulnar nerve and the disease causing cubital tunnel syndrome," *J. Shoulder Elb. Surg.* **17**(4), 585–588 (2008).
136. R. C. Ostrup et al., "Continuous monitoring of intracranial pressure with a miniaturized fiberoptic device," *J. Neurosurg.* **67**(2), 206–209 (1987).
137. P. Dario et al., "Fiber-optic catheter-tip sensor based on the photoelastic effect," *Sensor Actuat.* **12**(1), 35–47 (1987).
138. E. W. Saaski et al., "A family of fiber optic sensors using cavity resonator microshifts," in *4th Int. Conf. Optical Fiber Sensors*, pp. 11–14, Optical Society of America, Tokyo, Japan (1986).
139. K. D. Reesink et al., "Feasibility study of a fiber-optic system for invasive blood pressure measurements," *Catheter. Cardiovasc. Interv.* **57**(2), 272–276 (2002).
140. R. A. Wolthuis et al., "Development of a dual function sensor system for measuring pressure and temperature at the tip of a single optical fiber," *IEEE Trans. Bio-Med. Eng.* **40**(3), 298–302 (1992).
141. M.-D. Zhou et al., "An implantable Fabry-Pérot pressure sensor fabricated on left ventricular assist device for heart failure," *Biomed. Microdevices* **14**(1), 235–245 (2012).
142. C. Hamel and É. Pinet, "Temperature and pressure fiber optic sensors applied to minimally invasive diagnostics and therapies," *Proc. SPIE* **6083**, 608306 (2006).
143. A. Kolipaka et al., "MR elastography as a method for the assessment of myocardial stiffness throughout the cardiac cycle," in *Proc. Int. Soc. Mag. Reson. Med.*, p. 1790, MIRA, Digital Publishing, Honolulu, HI (2009).
144. M. Chavko et al., "Measurement of blast wave by a miniature fiber optic pressure transducer in the rat brain," *J. Neurosci. Methods* **159**(2), 277–281 (2007).
145. A. C. Leonardi et al., "Intracranial pressure increases during exposure to a shock wave," *J. Neurotrauma* **28**(1), 85–94 (2011).
146. A. Matsubara et al., "Investigating the effect of ciliary body photodynamic therapy in a glaucoma mouse model," *Invest. Ophth. Vis. Sci.* **47**(6), 2498–2507 (2006).
147. P. Zhang et al., "Knee loading dynamically alters intramedullary pressure in mouse femora," *Bone* **40**(2), 538–543 (2007).
148. S. Takeuchi et al., "An optic pharyngeal manometric sensor for deglutition analysis," *Biomed. Microdevices* **9**(6), 893–899 (2007).
149. C. A. Den Uil et al., "The effects of intra-aortic balloon pump support on macrocirculation and tissue microcirculation in patients with cardiogenic shock," *Cardiology* **114**(1), 42–46 (2009).
150. MAQUET, "Intra-aortic balloon catheters," (2011), http://ca.maquet.com/products/iab-catheters/ (10 May 2013).
151. P. Cottler et al., "Performance characteristics of a new generation pressure microsensor for physiologic applications," *Ann. Biomed. Eng.* **37**(8), 1638–1645 (2009).
152. K. Totsu et al., "Vacuum sealed ultra miniatue fiber-optic pressure sensor using white light interferometry," in *12th Int. Conf. Solid State Sensors, Actuators and Microsystems*, pp. 931–934, IEEE, Boston, MA (2003).

153. D. Donlagic and E. Cibula, "All-fiber high-sensitivity pressure sensor with SiO_2 diaphragm," *Opt. Lett.* **30**(16), 2071–2073 (2005).
154. E. Cibula and D. Donlagic, "Miniature fiber-optic pressure sensor with a polymer diaphragm," *Appl. Opt.* **44**(14), 2736–2744 (2005).
155. E. Cibula et al., "Miniature all-glass robust pressure sensor," *Opt. Express* **17**(7), 5098–5106 (2009).
156. E. Pinet, "Medical applications: saving lives," *Nat. Photon.* **2**(3),150–152 (2008).
157. FISO, "FOP-F125 product datasheet," http://www.fiso.com/admin/uploads/files/fop-f125.pdf (10 May 2013).
158. O. M. Sejersted et al., "Intramuscular fluid pressure during isometric contraction of human skeletal muscle," *J. Appl. Physiol.* **56**(2), 287–295 (1984).
159. L. Körner et al., "Relation of intramuscular pressure to the force output and myoelectric signal of skeletal muscle," *J. Orthop. Res.* **2**(3), 289–296 (1984).
160. M. Nakhostine et al., "Intramuscular pressure varies with depth: the tibialis anterior muscle studied in 12 volunteers," *Acta Orthop.* **64**(3), 377–381 (1993).
161. P. Peters et al., "Compartment syndrome following prolonged pelvic surgery," *Br. J. Surg.* **81**(8), 1128–1131 (1994).
162. I. Toft et al., "Quantitative measurement of muscle fiber composition in a normal population," *Muscle Nerve* **28**(1), 101–108 (2003).
163. K. A. Murphy et al., "Quadrature phase-shifted, extrinsic Fabry-Pérot optical fiber sensors," *Opt. Lett.* **16**(4), 273–275 (1991).
164. C. Willy et al., "Measurement of intracompartmental pressure with use of a new electronic transducer-tipped catheter system," *J. Bone Joint Surg. Am.* **81**(2), 158–68 (1999).
165. C. Yang et al., "Biocompatibility of a physiological pressure sensor," *Biosens. Bioelectron.* **19**(1), 51–58 (2003).
166. J. Davis et al., "Correlation between active and passive isometric force and intramuscular pressure in the isolated rabbit tibialis anterior muscle," *J. Biomech.* **36**(4), 505–512 (2003).
167. S. Chen et al., "Evaluating the dynamic performance of a fibre optic pressure microsensor," *Physiol. Meas.* **26**, N13–N19 (2005).
168. T. M. Winters et al., "Correlation between isometric force and intramuscular pressure in rabbit tibialis anterior muscle with an intact anterior compartment," *Muscle Nerve* **40**(1), 79–85 (2009).
169. K. N. An, "*In vivo* force and strain of tendon, ligament, and capsule," in *Functional Tissue Engineering*, F. Guilak, Eds., Vol. Part II, pp. 96–105, Springer, New York (2003).
170. J. R. Levick, "Joint pressure-volume studies: their importance, design and interpretation," *J. Rheumatol.* **10**(3), 353–357 (1983).
171. L. Mohanty and S. C. Tjin, "Pressure mapping at orthopaedic joint interfaces with fiber Bragg gratings," *Appl. Phys. Lett.* **88**(8), 083901 (2006).
172. P. K. Goh et al., "Measurement of intrameniscal forces and stresses by two different miniature transducers," *J. Mech. Med. Biol.* **7**(1), 65–74 (2007).
173. H. J. Wilke et al., "New *in vivo* measurements of pressures in the intervertebral disc in daily life," *Spine* **24**(8), 755–762 (1999).
174. B. W. Cunningham et al., "The effect of spinal destabilization and instrumentation on lumbar intradiscal pressure: an *in vitro* biomechanical analysis," *Spine* **22**(22), 2655–2663 (1997).
175. J.-L. Wang et al., "Interference in intradiscal pressure measurement using a needle-type pressure transducer," *J. Chin. Inst. Eng.* **30**(1), 149–153 (2007).
176. SAMBA, "Samba Preclin 420 and 360 transducer (discontinued)," www.sambasensors.com/products/preclinical-products/samba-preclin-420-360-transducer/ (11 November 2011).
177. S. Höejer et al., "A microstructure-based fiber optic pressure sensor for measurements in lumbar intervertebral discs," *Proc. SPIE* **3570**, 115–122 (1999).
178. H. Hebelka et al., "The transfer of disc pressure to adjacent discs in discography: a specificity problem?," *Spine* **35**(20), E1025–E1029 (2010).
179. T. Guehring et al., "Intradiscal pressure measurements in normal discs, compressed discs and compressed discs treated with axial posterior disc distraction: an experimental study on the rabbit lumbar spine model," *Eur. Spine J.* **15**(5), 597–604 (2006).
180. L. Ferrara et al., "A biomechanical assessment of disc pressures in the lumbosacral spine in response to external unloading forces," *Spine J.* **5**(5), 548–53 (2005).
181. L. Ekström et al., "*In vivo* porcine intradiscal pressure as a function of external loading," *J. Spinal Disord. Tech.* **17**(4), 312–316 (2004).
182. B. Hök et al., "Pressure microsensor system using a closed-loop configuration," *Sensor Actuat. A Phys.* **41**(1–3), 78–81 (1994).
183. A. H. Hsieh et al., "Intradiscal pressures in rat tail discs measured using a miniaturized fiber-optic sensor," *J. Biomech.* **39**(Suppl. 1), S28–S2490 (2006).
184. S. Nesson et al., "A miniature fiber optic pressure sensor for intradiscal pressure measurements of rodents," *Proc. SPIE* **6528**, 65280P (2007).
185. D. Hwang et al., "Role of load history in intervertebral disc mechanics and intradiscal pressure generation," *Biomech. Model Mechan.* **11**(1–2), 95–106 (2012).
186. D. J. Doyle and P. W. S. Mark, "Analysis of intracranial pressure," *J. Clin. Monitor Comput.* **8**(1), 81–90 (1991).
187. J. Piek and W. J. Bock, "Continuous monitoring of cerebral tissue pressure in neurosurgical practice: experiences with 100 patients," *Intensive Care Med.* **16**(3), 184–188 (1990).
188. J. K. Vries et al., "A subarachnoid screw for monitoring intracranial pressure," *J. Neurosurg.* **39**(3), 416–419 (1973).
189. M. Kosteljanetz et al., "Clinical evaluation of a simple epidural pressure sensor," *Acta Neurochir.* **83**(3), 108–111 (1986).
190. M. A. Poca et al., "Intracranial pressure monitoring with the Neurodur-P epidural sensor: a prospective study in patients with adult hydrocephalus or idiopathic intracranial hypertension," *J. Neurosurg.* **108**(5), 934–942 (2008).
191. A. Wald et al., "A new technique for monitoring epidural intracranial pressure," *Med. Instrum.* **11**(6), 352–354 (1977).
192. A. Wald, "Monitoring intracranial pressure," *J. Clin. Eng.* **3**(4), 383–388 (1978).
193. R. K. Narayan et al., "Experience with a new fiberoptic device for intracranial pressure monitoring," in *55th Annual Meeting American Association Neurological Surgeons*, American Association Neurological Surgeons, Dallas, TX (1987).
194. G. Gambardella et al., "Monitoring of brain tissue pressure with a fiberoptic device," *Neurosurgery* **31**(5), 918–922 (1992).
195. T. H. Smit et al., "Structure and function of vertebral trabecular bone," *Spine* **22**(24), 2823–2833 (1997).
196. AAMI, "Intracranial pressure monitoring devices," Vol. NS28, p. 10, ANSI/AAMI, Approved 17 November 1988 (2010).
197. S. L. Bratton et al., "VII. Intracranial pressure monitoring technology," *J. Neurotrauma* **24**(Suppl. 1), S45–S54 (2007).
198. M. Holzschuh et al., "Clinical evaluation of the InnerSpace fibreoptic intracranial pressure monitoring device," *Brain Inj.* **12**(3), 191–198 (1998).
199. OPSENS, "Fiber optic miniature pressure sensor," http://www.opsens.com/en/industries/products/pressure/opp-m/ (10 May 2013).
200. S. Sondergaard et al., "Direct measurement of intratracheal pressure in pediatric respiratory monitoring," *Pediatr. Res.* **51**(3), 339–345 (2002).
201. S. Sondergaard et al., "Fibre-optic measurement of tracheal pressure in paediatric endotracheal tubes," *Eur. J. Anaesth.* **18**, 24–25 (2001).
202. J. W. Arkwright et al., "A fibre optic catheter for simultaneous measurement of longitudinal and circumferential muscular activity in the gastrointestinal tract," *J. Biophoton.* **4**(4), 244–251 (2011).
203. R. A. De Blasi et al., "A fibre optics system for the evaluation of airway pressure in mechanically ventilated patients," *Intensive Care Med.* **18**(7), 405–409 (1992).
204. SAMBA, "Samba Resp 420 catheter (discontinued)," www.sambasensors.com/products/clinical-products/samba-resp-420-transducer/ (11 November 2011).
205. S. Voigt et al., "Homogeneous catheter for esophagus high-resolution manometry using fiber Bragg gratings," *Proc. SPIE* **7559**, 75590B (2010).
206. W.-C. Wang et al., "Development of a microfabricated optical bend loss sensor for distributive pressure measurement," *IEEE Trans. Bio-Med. Eng.* **55**(2), 614–625 (2008).
207. IASIS, "Intelligent adaptable surface with optical fiber sensing for pressure-tension relief," http://www.ist-world.org/ProjectDetails.aspx?ProjectId=ccaa7a17cf7b4d64a1a54702bafa64a4&SourceDatabaseId=018774364ea94468b3f4dec24aa1ee53 (10 May 2013).
208. G. Papaioannou et al., "Validation of a novel adaptive smart surface bed with integrated decubitus prophylaxis sensors," in *Proc. 56th Annual Meeting Orthopaedic Research Society*, Orthopaedic Reseach Society, New Orleans, LA (2010).

209. G. Papaioannou et al., "Towards a novel "SMARTsocket" design for lower extremity amputees," in *Proc HFM Symp. Advanced Technologies New Procedures Medical Field Operations*, NATO Science and Technology Organization, Essen, Germany (2010).
210. G. Papaioannou et al., "Assessment of vacuum-assisted trans-tibial amputee socket dynamics," in *Proc. 9th Int. Conf. Information Technology Applications Biomedicine*, IEEE, Larnaca, Cyprus (2009).
211. J. Z. Hao et al., "FBG-based smart bed system for healthcare applications," *Front Optoelectron. Chin.* **3**(1), 78–83 (2010).
212. J. R. Cobb and D. Claremont, "Transducers for foot pressure measurement: survey of recent developments," *Med. Biol. Eng. Comput.* **33**(4), 525–532 (1995).
213. R. P. Betts et al., "Critical light reflection at a plastic/glass interface and its application to foot pressure measurements," *J. Med. Eng. Technol.* **4**(3), 136–142 (1980).
214. C. I. Franks and R. P. Betts, "Selection of transducer material for use with 'optical' foot pressure systems," *J. Biomed. Eng.* **10**(4), 365–367 (1988).
215. C. Franks et al., "Microprocessor-based image processing system for dynamic foot pressure studies," *Med. Biol. Eng. Comput.* **21**(5), 566–572 (1983).
216. J. Z. Hao et al., "Design of a foot-pressure monitoring transducer for diabetic patients based on FBG sensors," in *16th Annual Meeting IEEE*, Vol. 1, pp. 23–24, IEEE, Tucson, AZ (2003).
217. W.-C. Wang et al., "A shear and plantar pressure sensor based on fiber-optic bend loss," *J. Rehabil. Res. Dev.* **42**(3), 315–325 (2005).
218. W.-C. Wang et al., "Optical and mechanical characterization of microfabricated optical bend loss sensor for distributive pressure measurement," in *Health Monitoring Structural and Biological Systems 2007*, pp. 65321K, SPIE, San Diego, CA (2007).
219. W.-C. Wang et al., "Transducing mechanical force by use of a diffraction grating sensor," *Appl. Opt.* **45**(9), 1893–1897 (2006).
220. W. Soetanto et al., "Fiber optic plantar pressure/shear sensor," *Proc. SPIE* **7984**, 79840Z (2011).